Laboratory Seismic Testing of Asphalt Concrete

Anders Gudmarsson

Licentiate Thesis

KTH Royal Institute of Technology

School of Architecture and Built Environment

Department of Transport Science

Division of Highway and Railway Engineering

SE-100 44 Stockholm

Stockholm 2012

TRITA-TSC-LIC 12-009

ISBN 978-91-85539-97-0

Acknowledgement

This thesis is a result of the collaboration initiated by Lennart Holmqvist, Nils Ryden and Björn Birgisson between Peab Asfalt AB and the division of Highway and Railway Engineering at KTH Royal Institute of Technology.

The Swedish construction industry's organization (SBUF) and the Swedish Transport Administration (Trafikverket) are gratefully acknowledged for the financing of this project.

I would like to express my sincere gratitude to my supervisor Nils Ryden for all his time and knowledge spent on this project. I am very thankful for all the support and help he has given me so far. My supervisor Björn Birgisson is also gratefully acknowledged for his excellent feedback and insights to this project.

I am very thankful to Lennart Holmqvist and to my colleagues at Peab Asfalt AB for their great support before and during this project.

Thanks also to my colleagues at KTH for good discussions and for any help given when needed. Agneta Arnius is also gratefully acknowledged for her good support.

Thanks to the participants of the Friday meeting group and to the members of the reference group for valuable feedback and help regarding this project.

Finally, I would like to thank my family and friends for supporting and helping out during my years of studying.

Anders Gudmarsson

Stockholm, September 2012

Abstract

Nondestructive laboratory seismic testing to characterize the complex modulus and Poisson's ratio of asphalt concrete is presented in this thesis. These material properties are directly related to pavement quality and the dynamic Young's modulus is used in thickness design of pavements. Existing standard laboratory methods to measure the complex modulus are expensive, time consuming, not truly nondestructive and cannot be directly linked to nondestructive field measurements. This link is important to enable future quality control and quality assurance of pavements based on the dynamic modulus. Therefore, there is a need for a more detailed and accurate laboratory test method that is faster, more economic and can increase the understanding and knowledge of the behavior of asphalt concrete. Furthermore, it should be able to be linked to nondestructive field measurements for improved quality control and quality assurance of pavements.

Seismic testing can be performed by using ultrasonic measurements, where the speed of sound propagating through a material with known dimensions is measured. Seismic testing can also be used to measure the resonance frequencies of an object. Due to any excitation, a solid resonates when the frequency of the applied force matches the natural frequencies of the object. In this thesis, resonance frequency measurements have been performed at several different temperatures by applying a load impulse to a specimen while measuring its dynamic response. The measured resonance frequencies and the measured frequency response functions have been used to evaluate the complex modulus and Poisson's ratio of asphalt concrete specimens. Master curves describing the complex modulus as a function of temperature and loading frequency have been determined through these measurements.

The proposed seismic method includes measurements that are significantly faster, easier to perform, less expensive and more repeatable than the conventional test methods. However, the material properties are characterized at a higher frequency range compared to the standard laboratory methods, and for lower strain levels ($\sim 10^{-7}$) compared to the strain levels caused by the traffic in the pavement materials.

Importantly, the laboratory seismic test method can be linked together with nondestructive field measurements of pavements due to that the material is subjected to approximately the same loading frequency and strain level in both the field and laboratory measurements. This allows for a future nondestructive quality control and quality assurance of new and old pavement constructions.

Sammanfattning

I denna avhandling presenteras oförstörande seismisk laboratorieprovning för att bestämma asfaltprovkroppars komplexa styvhetsmodul och tvärkontraktionstal. Dessa materialegenskaper är direkt kopplade till beläggningars kvalitet och den dynamiska styvhetsmodulen används vid dimensionering av vägar. De traditionella laboratoriemetoderna för att bestämma den komplexa styvhetsmodulen är kostsamma, tidskrävande, inte helt oförstörande och kan inte jämföras med resultat från oförstörande fältmätningar. Länken mellan laboratorieprovning och fältmätningar är synnerligen viktigt för att möjliggöra en modern kvalitetskontroll av asfaltbeläggningar baserad på den dynamiska styvhetsmodulen. Det finns därför ett stort behov av en noggrannare laboratoriemetod som är tids- och kostnadseffektiv samt kan bidra till en ökad förståelse och kunskap om asfalts egenskaper. Metoden ska även kunna kopplas till oförstörande fältmätningar för att kunna förbättra kvalitetskontrollerna av vägkonstruktioner.

Seismisk provning kan utföras genom ultraljudsmätningar där hastigheten av vågor som propagerar genom ett material med kända dimensioner mäts upp. Mätning av ett objekts resonansfrekvenser är också ett exempel på seismisk provning. När en kropp utsätts för en extern kraft som motsvarar objektets egenfrekvenser uppstår resonans. I denna avhandling har resonansfrekvensmätningar utförts vid ett flertal olika temperaturer genom att excitera en asfaltprovkropp och mäta dess dynamiska respons. Uppmätta resonansfrekvenser och frekvensresponsfunktioner har använts för att utvärdera komplexa styvhetsmoduler och tvärkontraktionstal för asfaltprovkroppar. Masterkurvor som beskriver den komplexa styvhetsmodulen som funktion av temperatur och belastningsfrekvens har bestämts utifrån dessa mätningar.

I jämförelse med de traditionella mätmetoderna kan mätningar av den komplex styvhetsmodulen utföras enklare, snabbare och mer kostnadseffektivt med den föreslagna seismiska laboratoriemetoden. Dessutom är seismiska mätmetoder betydligt mer repeterbara än de traditionella metoderna. Materialegenskaperna mäts dock vid högre belastningsfrekvenser och lägre töjningsnivåer (~10^{-7}) än vad en trafikbelastad beläggning utsätts för i fält.

Resultat från oförstörande seismiska fältmätningar kan direkt jämföras med resultat från den seismiska laboratoriemetoden tack vare att materialet utsätts för samma belastningsfrekvens och töjningsnivåer i dessa testmetoder. Detta möjliggör en framtida oförstörande kvalitetskontroll av nya och gamla vägkonstruktioner baserad på den dynamiska styvhetsmodulen.

Papers

This thesis is based on the following papers:

Paper I. Gudmarsson, A., Ryden, N., Birgisson, B., 2012, Application of resonant acoustic spectroscopy to asphalt concrete beams for determination of the dynamic modulus, *Materials and Structur*es, DOI: 10.1617/s11527-012-9877-3.

Paper II. Gudmarsson, A., Ryden, N., Birgisson, B., 2012, Characterizing the low strain complex modulus of asphalt concrete specimens through optimization of frequency response functions, *Journal of Acoustical Society of America*, Vol. 132, Issue 4, pp. 2304-2312.

Related publications

Gudmarsson, A., Ryden, N., Birgisson, B., 2010, Application of resonant acoustic spectroscopy to beam shaped asphalt concrete samples, *Journal of Acoustical Society of America*, Vol. 128, Issue 4, pp. 2453.

Gudmarsson, A., Ryden, N., Birgisson, B., 2011, Determination of the frequency dependent dynamic modulus for asphalt concrete beams using resonant acoustic spectroscopy, *Nondestructive Testing of Materials and Structures, Proceedings of NDTMS-2011, Istanbul, Turkey, RILEM Bookseries*, Vol. 6, DOI: 10.1007/978-94-007-0723-8.

Gudmarsson, A., Ryden, N., Birgisson, B., 2012, Nondestructive evaluation of the complex modulus master curve of asphalt concrete specimens, accepted for publication in *Review of Progress in Quantitative Nondestructive Evaluation, American Institute of Physics Conference Proceedings*.

Table of Contents

1. Introduction

The magnitude of the strain level at the bottom of asphalt concrete layers is currently used in thickness design of pavements in Sweden. At this date, the strains are estimated through an empirical approach by using tables of the stiffness of the material. These tables account for the type of asphalt mixture and climate conditions but are not specific for the actual materials used in the pavement construction (TRVK Väg 2011). Therefore, there is a great interest to use a more analytical approach of predicting the upcoming stresses and strains in the materials used in pavement constructions.

Furthermore, today's control of pavement quality is based on coring to investigate the air void content and thickness of the asphalt layer. The air void content in the cored specimens is used as a measure of the packing quality for new pavement constructions, since it may indicate if the correct stiffness has been achieved. However, there is no parameter investigated that could be directly related to the stiffness of the material. Quality control based on a direct relation to the stiffness would provide a better knowledge of the true behavior of the material.

The dynamic Young's modulus of asphalt concrete is one of the main inputs in thickness design of pavements. Due to the viscoelastic nature of asphalt concrete, a master curve is can be used to characterize the viscoelastic complex modulus over a range of temperatures and frequencies. The estimation of a master curve requires a nondestructive testing technique to be able to measure the complex modulus of a specimen at several different temperatures and loading frequencies. However, the existing standard laboratory test methods to measure the complex modulus are not truly nondestructive (Brown et al. 2009). This limitation affects the test procedure of the traditional methods in order to cause as little damage as possible to the tested specimens. For example, the test sequence starts at the lowest test temperature and highest frequency and goes towards higher temperatures and lower frequencies. The traditional methods are performed by applying a cyclic load to the specimen while measuring the deformation of the specimen. The methods require relatively heavy equipment to apply the load and sensitive strain-gauges to measure the deformation. Hence, expensive equipment is needed and it is often time-consuming to perform the necessary settings to measure the complex modulus. The traditional methods sensitivity to the test set-up may also reduce the repeatability and reproducibility of these tests. Still, it is of great interest to be able to construct asphalt concrete master curves, due to its ability to express the complex modulus over a wide range of temperatures and frequencies. Master curves can also provide a great support in the development of new improved asphalt mixtures. There is therefore a need for a simpler, faster and more accurate method that is truly nondestructive to determine the complex modulus master curve of asphalt concrete specimens.

Resonance frequencies of all free solids depend on the dimensions, mass and stiffness of the object. Therefore, it is possible to determine the stiffness of a material through measurements of the solids resonance frequencies, mass and dimensions. Measurements of resonance frequencies to extract material properties are widely used in other fields of engineering and are often referred to as resonant ultrasound spectroscopy (Migliori and Sarrao 1997) or resonant acoustic spectroscopy (Ostrovsky et al. 2001). Resonance testing has also been applied to asphalt concrete specimens in several studies (e. g. Whitmoyer and Kim 1994; Kweon and Kim 2006; Lacroix et al. 2009). However the results from these measurements have been based on a simplified approach of calculating the modulus of the specimens (ASTM C215 2008). This has limited the determination of the complex modulus to the fundamental resonance frequency for different modes of vibration at each testing temperature. It has therefore not been possible to construct master curves using only results obtained from the resonance frequency testing in these studies.

This thesis presents the development of truly nondestructive testing techniques based on seismic measurements. The aim of this study has been to develop a nondestructive measurement technique to be able to determine the complex modulus master curve of asphalt concrete specimens.

2. Summary of papers

The papers appended in this thesis present methods of evaluating seismic measurements to characterize the complex moduli of asphalt concrete specimens. Paper I presents the approach of resonant acoustic spectroscopy (RAS) and how it can be applied to viscoelastic materials. The presented complex moduli are calculated for the resonance frequencies of the specimens only. Paper II expands the usable frequency range by the use of frequency response functions (FRFs), where theoretical FRFs are optimized against measured FRFs.

Paper I: Application of resonant acoustic spectroscopy to asphalt concrete beams for determination of the dynamic modulus

The response of a specimen due to an impact is measured and used to determine the resonance frequencies of the specimens. The complex moduli are estimated through energy minimization techniques including the Rayleigh-Ritz approximation and an iterative procedure of matching theoretical against measured resonance frequencies. The complex modulus is determined for each resonance frequency and mode type. Binder shift factors are used to characterize the dynamic modulus master curve.

Paper II: Characterizing the low strain complex modulus of asphalt concrete specimens through optimization of frequency response functions

The force of the impact and the response of the specimen are measured to determine the frequency response functions (FRFs) of the specimen at different temperatures. Theoretical FRFs are determined through the finite element method. An optimization process is developed to match theoretical FRFs with the measured FRFs to extract the material properties. The complex modulus master curve is constructed using only seismic measurements.

3. Theory and measurement techniques of the complex modulus

The properties of viscoelastic materials like asphalt concrete depend strongly on temperature and loading frequency. Each type of asphalt concrete mixture has unique viscoelastic properties and testing of the material must therefore be performed at different temperatures and loading frequencies for each mixture. A numerous types of analysis are often performed to asphalt concrete. However, this thesis focuses on methods for complex modulus testing of asphalt concrete specimens.

3.1 Traditional methods to measure the complex modulus

There are three different standard laboratory test methods available today to measure the complex modulus of asphalt concrete specimens. They are the *AASHTO TP-62 Standard Method of Test for Determining Dynamic Modulus of Hot-Mix Asphalt Concrete Mixtures* (TP 62), the *Asphalt Mixture Performance Tester* (AMPT) and the *Indirect Tension* (IDT) complex modulus test. The TP 62 and AMPT tests both require cylindrical specimens with a diameter and height of approximately 100 mm and 150 mm, respectively. In these tests a sinusoidal load is applied in the direction of the axis of the height and 2, 3 or 4 LVDTs measure the axial deformation. The load is applied at six different loading frequencies between 0.1 to 25 Hz using the TP 62 test protocol and at four different frequencies between 0.01 to 10 Hz using the AMPT test protocol. For both the TP 62 and the AMPT test, the magnitude of the applied load and the cross-sectional area of the specimen are used to determine the applied stress (σ) to the specimen. The applied strain (ε) is determined through the axial deformation of the specimen and the gauge length. The dynamic modulus of the specimen can thereafter be calculated according to Eqn. 1 and the phase angle according to Eqn. 2.

$$\left|E^*\right| = \frac{\sigma_0}{\varepsilon_0} \tag{1}$$

where $|E^*|$ = dynamic modulus [Pa],
σ_0 = peak-to-peak stress amplitude [Pa],
ε_0 = peak-to-peak strain amplitude [-].

$$\phi = 2\pi f \Delta t \tag{2}$$

where ϕ = phase angle [rad],
f = frequency [Hz],
Δt = time lag between stress and strain [s].

The dynamic modulus and the phase angle relate to the complex modulus according to Eqn. 3.

$$E^* = \left|E^*\right| \cdot e^{i\phi} \tag{3}$$

The complex modulus can also be expressed by the storage and loss modulus according to Eqn. 4, where the storage modulus represent the elastic energy and the loss modulus represent the viscous energy.

$$E^* = E' + iE'' \tag{4}$$

where E' = storage modulus,
E'' = loss modulus,
i = the complex number.

Furthermore, the phase angle can also be expressed by the loss and storage modulus according to Eqn. 5.

$$\phi = \tan^{-1}\left(\frac{E''}{E'}\right) \tag{5}$$

Fig. 1 shows an example of equipment that can be used to measure the complex modulus for the TP 62 and AMPT test methods.

Fig. 1 Equipment to measure the complex modulus of asphalt concrete using the TP 62 and AMPT standard test methods

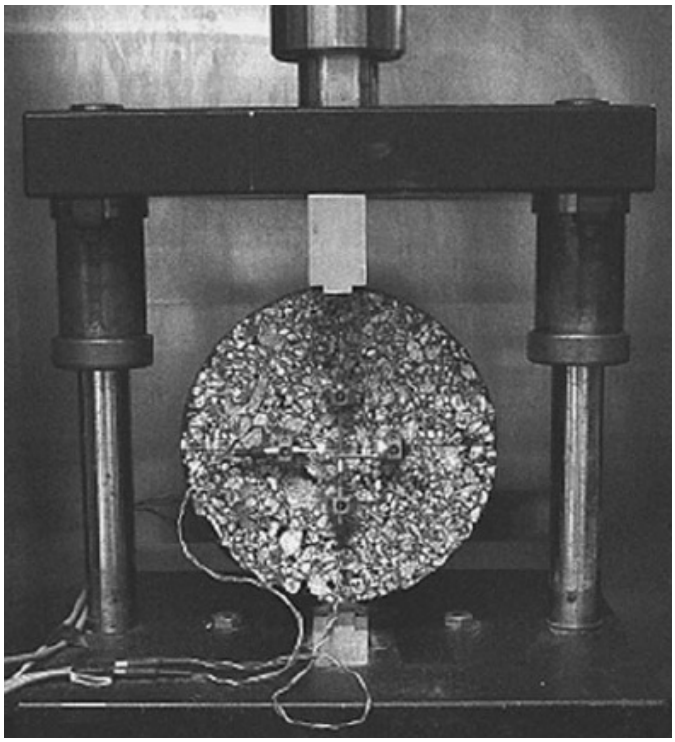

Fig. 2 Test set-up for the IDT complex modulus test, measuring both vertical and horizontal deformations (Kim et al. 2004)

The IDT complex modulus test was developed to be able to use more easily obtained specimens than what the TP 62 and AMPT tests require. The specimen dimensions used in the TP 62 and AMPT test protocols are most often not possible to obtain from coring in real pavements. The IDT complex modulus test protocol reported by Kim et al. (2004) applies eight loading frequencies between 0.01 to 25 Hz. The test protocol uses disc-shaped specimens with a diameter and thickness of approximately 150 mm and 40 mm, respectively. As a consequence of this geometry, the sinusoidal load is applied perpendicular to the actual compaction direction of the specimen, whereas the TP 62 and AMPT tests apply the load in the same direction as the compaction. Furthermore, the stress state in the IDT test becomes biaxial instead of uniaxial (as it is in the other test methods) and the deformations needs to be measured in both the horizontal and the vertical direction (see Fig. 2). Therefore, the calculation of the dynamic modulus requires additional terms to account for the displacements in two directions and the geometry of the specimen. The dynamic modulus from the IDT tests is calculated according to Eqn. 6 (Kim et al. 2004).

$$\left|E^*\right| = 2\frac{P_0}{\pi a d}\frac{\beta_1\gamma_2 - \beta_2\gamma_1}{\gamma_2 V_0 - \beta_2 U_0} \tag{6}$$

where P_0 = applied load amplitude [N],
a = width of loading strip [m],
d = thickness of specimen [m],
V_0 = average vertical displacement magnitude [m],

U_0 = average horizontal displacement magnitude [m],
β_1, β_2, γ_1, γ_2 = geometric coefficients [-].

3.2 Master curves

A master curve can be constructed for materials that are thermorheologically simple (Brown et al. 2009). Thermorheologically simple materials can have the same behavior at high loading frequencies and high temperatures as they have at lower loading frequencies and lower temperatures. For these materials it is possible to predict the same value of the modulus at a different temperature and frequency, than for which it was actually measured. This is performed by applying the time-temperature superposition principle (TTSP) to the measured modulus. By applying the TTSP a measured modulus is shifted horizontally until its value coincides with a modulus measured at another temperature and frequency (see Fig. 3 and 4). The shifted modulus then becomes a function of a reference temperature and reduced frequency. The application of the TTSP requires that there is an overlap of the modulus between the different measured temperatures. An example of the dynamic modulus measured at different temperatures and loading frequencies is presented in Fig. 3.

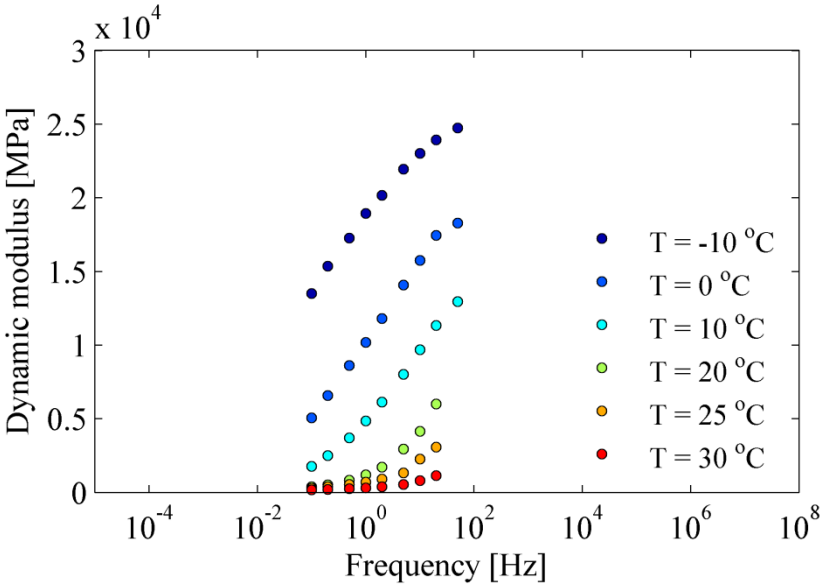

Fig. 3 The dynamic modulus measured at different loading frequencies and temperatures

In Fig. 3 it can be seen that the modulus is measured between minimum 0.1 Hz to maximum 50 Hz and that there is an overlap of the measured dynamic modulus between the temperatures. From these measurements it is possible to construct a master curve by shifting for example the measured modulus at -10, 0, 20, 25 and 30 °C to a single continuous curve at 10 °C. Fig. 4 shows the measured dynamic modulus that has been shifted to a single continuous master curve over a wide reduced frequency at a reference temperature of 10 °C.

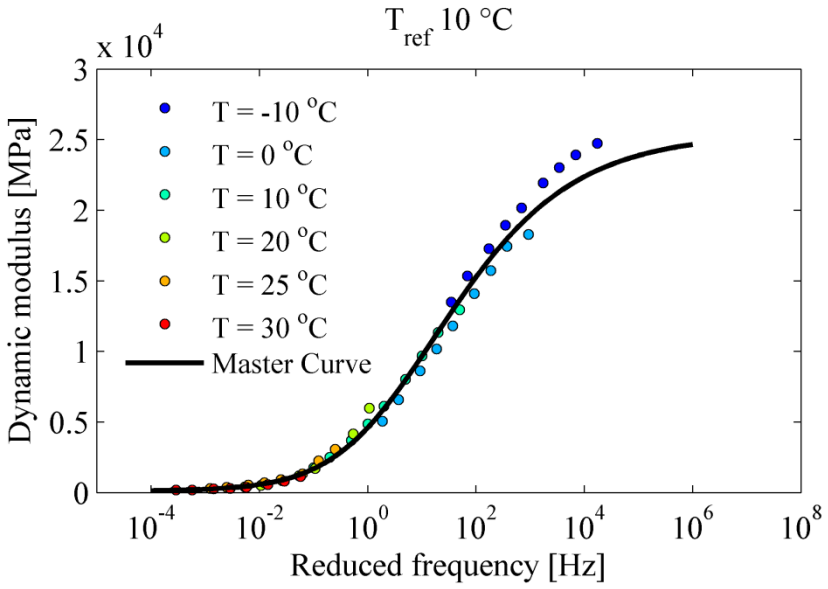

Fig. 4 The dynamic modulus master curve at a reference temperature of 10 °C

The shift factors ($\alpha(T)$), which is a measure of the temperature dependency of the material, are often calculated by using the Williams-Landel-Ferry equation (Eqn. 7) (Williams et al. 1955).

$$\log \alpha(T) = \frac{-c_1(T - T_{ref})}{c_2 + T - T_{ref}} \tag{7}$$

where c_1, c_2 = material constants [-],
T = reference temperature [°C],
T_{ref} = temperature [°C].

The reduced frequencies (f_{red}) are obtained by multiplying the shift factors with the loading frequency (f) according to Eqn. 8.

$$f_{red} = \alpha(T)\, f \tag{8}$$

The sigmoidal function (Eqn. 9), that is commonly applied to asphalt concrete, shows how the analytical dynamic modulus master curve can be calculated.

$$\log\left|E^*\right| = \delta + \frac{\alpha}{1 + e^{\left(\beta - \gamma \log\left(f_{red}\right)\right)}} \tag{9}$$

where δ, α, β, γ = material constants [-],
f_{red} = reduced frequency [Hz].

The master curve and the shift factors are determined by adjusting the unknown material constants δ, α, β, γ, c_1 and c_2 until the analytical dynamic modulus (Eqn. 9) matches the measured dynamic modulus. The procedure of estimating unknown constants applies for

any relationship that is used to characterize the dynamic or complex modulus master curve of asphalt concrete by comparison against measured complex modulus data.

3.3 Seismic measurements

Mechanical waves are waves that propagate through a medium in which the energy of the waves is transferred through the connected particles. Seismic, acoustic and sound waves are all examples of mechanical waves. Seismic waves include two types of waves, body waves and surface waves. Body waves can propagate longitudinally or transversely in an infinite medium. The longitudinal waves which are compressional waves are the fastest propagating waves and are therefore called for primary waves (P-waves). The transverse waves which are shear waves are called secondary waves (S-waves) since they propagate slower and always arrive after the P-wave. Surface waves that propagate along a free surface of a homogenous half space are generally either of the Rayleigh or the Love type of waves. Waves propagating in a free homogenous plate are called Lamb waves, which are important for seismic field testing of pavements.

Compression waves propagate with the speed of sound, which depend on the medium they travel through. The general relationship describing the speed of sound (v) propagating through a medium in a linear system is given by Eqn. 10, where C_{ij} is the elastic component related to the direction of the wave propagation and ρ is the density.

$$v = \sqrt{\frac{C_{ij}}{\rho}} \tag{10}$$

Consequently, by measuring the time and distance of a wave propagating through a solid with a certain density the elastic properties of the solid can be determined. This basic relation has been utilized to develop nondestructive ultrasonic testing techniques in many fields of engineering (cf. e.g. Popovics and Rose 1994; Leisure and Willis 1997). Among the most common techniques is the pulse velocity method, which has been used since the 1940's to evaluate elastic properties of rocks and concrete (Popovics and Rose 1994). In the test, the time of flight of a wave propagating through e. g. concrete with known thickness is measured. Usually a source and a receiver are positioned on each side of the material to excite the wave propagation and to measure the arrival time. Another common technique is pulse-echo methods where the source and the receiver are located at the same side and measures the time of the echo to return from opposite surfaces.

Nazarian et al. (2005), Di Benedetto et al. (2009) and Norambuena-Contreras et al. (2010) have all applied ultrasonic measurements to asphalt concrete specimens to determine the modulus. However, some important disadvantages applying ultrasonic methods to asphalt concrete are that the modulus is determined at very high frequencies (> 20 kHz) and that the modulus has only been determined for one frequency at each test temperature. It is important to be able to determine the complex modulus of asphalt

concrete over a wider frequency range including low frequencies, since knowledge of the low frequency modulus is significant for pavement response analysis. The main disadvantage is although caused by the inhomogeneity of asphalt concrete. The accuracy of the ultrasonic testing decreases when it is applied to materials that are not truly homogeneous.

Measurement of resonance frequencies is another seismic method that can be applied to determine elastic constants of solids. A solid or a system resonates when the frequency of an external force matches the natural frequency or frequencies of the object. Resonance frequencies of a solid depend on the stiffness, mass, dimension and the boundary conditions. Hence, by controlling the boundary conditions and measuring a solid's resonance frequencies, mass and dimensions, the elastic constants of the solid can be determined. Measurements of resonance frequencies are today widely considered as one of the most accurate methods to determine elastic constants (Li and Gladden 2010). Especially, the development of resonant ultrasound spectroscopy (RUS) has proven to be a very accurate and efficient method to determine elastic constants (Migliori et al. 1993; Migliori and Sarrao 1997). RUS includes detailed measurements of resonance frequencies, the forward problem of calculating theoretical resonance frequencies and the inverse problem where the assumed elastic constants are adjusted until the theoretical resonance frequencies matches the measured ones. The calculation of theoretical frequencies is performed by minimizing the Lagrangian and by using the Rayleigh-Ritz approximation to expand the displacement vector in terms of basis functions in order to evaluate the displacements numerically (Migliori and Sarrao 1997). This calculation require the assumptions of stress-free boundary conditions and simple harmonic motion which means that it is the natural resonance frequencies without any damping that are being calculated. The development of RUS is relatively new compared to the wave propagation techniques, due to need of computers for efficient calculation of the forward and inverse problem. Before Holland (1967) and Demarest (1971) applied numerical approximation methods to calculate theoretical resonance frequencies, the analytical calculations were limited to specific geometries as cubes or spheres. Ohno (1976) refined and extended the work performed by Demarest to determine elastic constants for further symmetries and these papers provided a base for the development of the technique that is today called RUS, or resonant acoustic spectroscopy (RAS) when it is applied in a lower frequency range up to 20 kHz (Ostrovsky et al. 2001). Note that this development of RUS and RAS can be applied to arbitrary geometries by using e.g. powers of Cartesian coordinates as basis functions (Visscher et al. 1991).

Comparing the two seismic methods of speed of sound and resonance frequency measurements, the latter method often provide important advantages in speed and accuracy. Wave propagation methods are usually based on the approximation of plane-waves which are sensitive to diffraction effects that limits the accuracy of the measurements. For example, the more heterogeneous the material is, the more the propagating waves deviate from the assumption of plane-waves. This deviation gets

worse for the higher the frequencies are, that are applied in the test. Since there is no plane-wave approximation when evaluating resonance frequency measurements, and since lower frequencies can be applied the accuracy is higher. The plane-wave assumption also limits how small the specimens can be since the oscillating wavelength needs to be much smaller than the specimen. There is almost no limit of the size of the object that RUS can be applied to. Another important advantage is that using resonance frequency measurements it is possible to determine the complete stiffness coefficient matrix from one single measurement. The number of measurements needed to obtain the same result using wave propagation methods is at least equal to the number of stiffness coefficients in the matrix (Leisure and Willis 1997).

Resonance frequency measurements of asphalt concrete specimens evaluated analytically using the concrete standard ASTM C215 has been reported in several papers (cf. e. g. Whitmoyer and Kim 1994, Kweon and Kim 2006, Lacroix et al. 2009). The fundamental modes of vibration are used to determine the material properties of specimens using the ASTM C215 standard (ASTM C215 2008). This means that it is only possible to determine one modulus per measurement temperature. Although these results have shown a promising agreement with conventional testing of the complex modulus, they cannot be used alone to characterize the material properties over a wide frequency range. It is therefore not possible to determine master curves from these results only. Through the use of RAS it is on the other hand possible to determine the material properties at several resonance frequencies and not only for the fundamental resonance frequency. This opens up the possibility of being able to estimate master curves using only seismic testing. However, at higher resonance frequencies it may be difficult to make sure that the correct theoretical resonance frequency are matched against the corresponding measured resonance frequency. This is due to that resonance frequencies of different modes of vibration at higher frequencies may be difficult to differentiate. This mode identification issue may limit the amount of usable resonance frequencies available for the material characterization. The application of RAS to asphalt concrete specimens is explained in more detail in paper I.

In general it may difficult to determine master curves of material properties using only the resonance frequencies of viscoelastic objects. In the case of asphalt concrete specimens it may in some cases only be possible to measure three or four resonance frequencies to determine the complex modulus, which is usually not enough to estimate a master curve. For viscoelastic materials it is therefore useful to be able to characterize the material properties in a more closely spaced frequency interval than what resonances can provide. This can be accomplished by using measured frequency response functions (FRFs) instead of only the measured resonance frequencies (Ren et al. 2011; Renault et al. 2011; Rupitsch et al. 2011). A FRF is determined by normalizing the measured response of a specimen with the measured applied load in frequency domain. Note that the same testing can be performed to measure the resonance frequencies and to determine the FRFs. However, by accounting for the applied load it becomes possible to use the

whole response curve to estimate the material properties instead of the resonance peaks only (see Fig. 5). Figure 5 shows a measured FRF at -1.6 °C for the longitudinal modes of vibration of a beam-shaped asphalt concrete specimen, where the peaks are the resonance frequencies that are used to estimate the material properties when applying RAS. The FRF has been determined by the following relationship,

$$H(f) = \frac{Y(f) \times X^*(f)}{X(f) \times X^*(f)}, \tag{11}$$

where $H(f)$ = the frequency response function,
$Y(f)$ = the measured response,
$X(f)$ = the measured applied force,
$X^*(f)$ = the complex conjugate of the applied force.

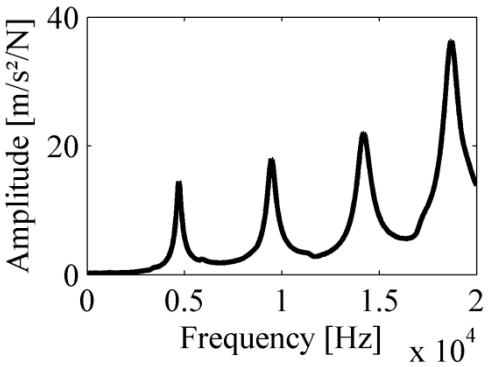

Fig. 5 The measured frequency response function at -1.6 °C for the longitudinal modes of vibration of a beam-shaped asphalt concrete specimen.

Through the use of FRFs, the complex modulus of asphalt concrete specimens can be estimated by optimizing theoretical FRFs against measured FRFs, where the assumed material properties are adjusted until a good match is obtained. The theoretical FRFs can be calculated either analytically (Quo and Brown 2001; Renault et al. 2011) or numerically by using e. g. the finite element method (Rupitsch et al. 2011). The method of optimizing FRFs to characterize the complex moduli of asphalt concrete specimens is more thoroughly presented in paper II.

3.4 QC/QA through seismic testing

Seismic field measurements can be used to estimate the stiffness and thickness of the different layers in a pavement construction (Nazarian 1993; Nazarian 1999; Ryden 2004). This is performed by measuring the phase velocity of dispersive guided Lamb waves generated by applying a load impulse to the surface of the pavement structure. Due to the free surface and the different layers of a pavement structure, guided waves (surface waves) are formed when P and S-waves interact at the interfaces of the different layers. The propagation of guided Lamb waves is therefore dependent on the stiffness

and thickness of the different layers making them very useful for characterization of pavement structures. The guided Lamb waves are dispersive which means that the phase velocity of the propagating waves is frequency dependent. This relation between phase velocity and frequency can be described by dispersion curves. Stiffness and thickness of the layers in the structure are estimated by calculating theoretical dispersion curves that are iteratively matched against measured dispersion curves until the adjusted theoretical layer model provides dispersion curves that match the measured ones.

Results from seismic field measurements of pavements can be directly linked to seismic laboratory measurements due to that the material is subjected to approximately the same loading frequency and strain level in both the field and laboratory measurements. As an example, a modulus measured at any temperature in the field can be directly compared to a master curve that has been estimated for a laboratory produced specimen through seismic laboratory testing. This allows for nondestructive quality control and quality assurance of new and old pavement constructions.

Figure 6 illustrates the use of a master curve as a tool for quality control and quality assurance of pavements. In this example, a master curve has been determined through laboratory seismic testing and upper and lower limits of the dynamic modulus have been determined in the design of the pavement. By performing seismic field measurements at any temperature within the presented interval and at the frequency of 500 Hz, the resulting dynamic modulus can be compared to the laboratory determined master curve and to the design requirements.

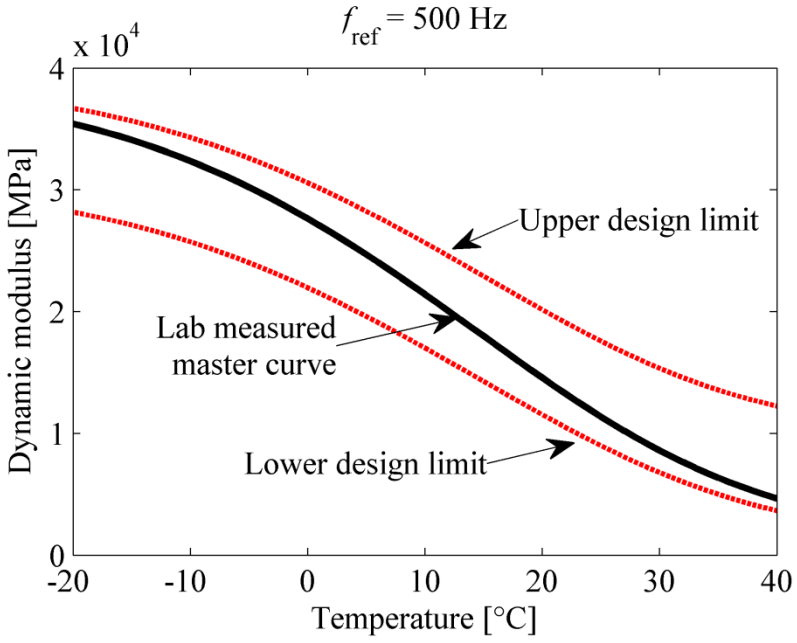

Fig. 6 Illustration of quality control of pavements using a seismic laboratory determined master curve and seismic field measurements.

4. Results and discussion

Both RAS and optimization of FRFs to evaluate seismic measurements applied to beam-shaped asphalt concrete specimens are presented in the appended papers. This chapter presents a summary of the results obtained from both of these methods. All of the results presented in this thesis are based on the assumption that the material is isotropic, linear viscoelastic and homogenous. These assumptions imply that the material has the same stiffness in both tension and compression (i.e. flexural and longitudinal modes of vibration) and that the behavior of the material can be described by a complex modulus and Poisson's ratio.

The seismic measurements providing the results presented here were performed by placing a beam-shaped specimen (382, 58.74, 58.94 mm) on soft foam and applying a load impulse exciting the longitudinal modes of vibration. An instrumented hammer was used to apply the load and an accelerometer was used to measure the dynamic response of the specimen. These measurements were performed at 11 different temperatures (-24.4, -20.5, -15.1, -10.5, -5.4, -1.6, 5.4, 11.3, 15.8, 20.5 and 30.1 °C).

Applying RAS can provide characterization of the elastic constants of the material, which provides information of the real part (storage modulus) of the complex modulus. In order to account for the viscoelastic properties of the material, RAS needs to be supplemented with a method to characterize the intrinsic damping of the material, which can give information of the imaginary part (loss modulus). In this approach, RAS is combined with the half-power bandwidth method to be able to estimate the damping and hence, the complex modulus of the asphalt concrete specimens. However, the half-power bandwidth method has been shown to be sufficiently accurate only as long as the damping ratio is below approximately 0.1, corresponding to a phase angle of approximately 11 ° (Wang et al. 2012). Note that when using FRFs the estimation of the damping is included in the optimization process through the direct characterization of the complex modulus.

The results of the dynamic moduli of a beam-shaped asphalt concrete specimen estimated using RAS and FRFs are presented in figure 7. The RAS determined dynamic modulus is presented for the first two resonance frequencies for all measurement temperatures except 30.1 °C, where the damping was too high to be able to apply the half-power bandwidth method.

The complex modulus determined through the optimization of FRFs has been performed by using two different optimization approaches. First, an optimization process has been performed for each measured FRF at the different temperatures giving results of the complex modulus at each temperature separately. Secondly, FRFs of all measurement temperatures have been used in one global optimization process leading to a direct

estimation of the complex modulus master curve. As can be seen in figure 7, the two optimization approaches of the FRFs provide very similar results of the dynamic moduli. The dynamic moduli results from RAS are also similar to the FRF results at the lower temperatures while a small difference can be found as the temperature increases.

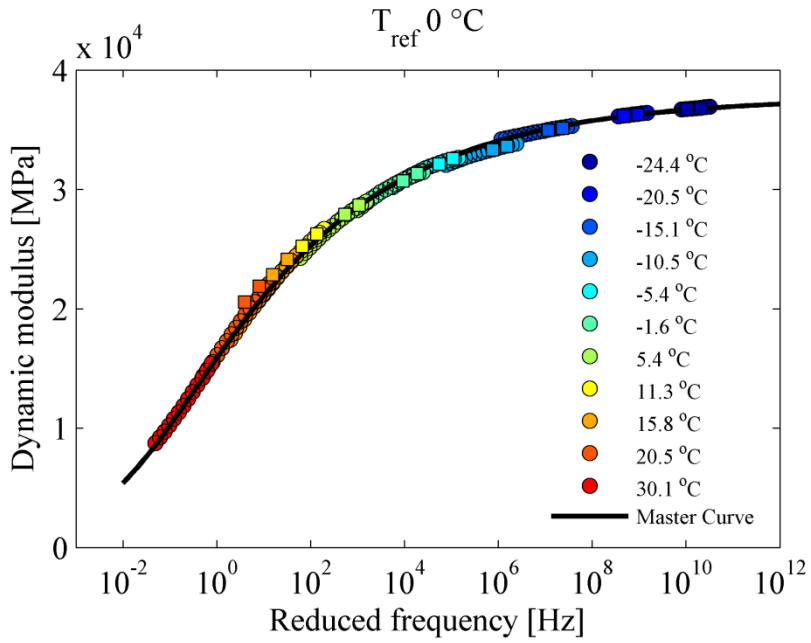

Fig. 7 The dynamic moduli determined by RAS – □, separate optimization of the FRFs – ○ and global optimization of the FRFs (master curve).

This difference between RAS and FRFs is seen more clearly when presenting the estimated phase angle in figure 8, where the RAS determined phase angle has been estimated through the use of the half-power bandwidth method. In figure 8, the phase angle results of the FRF optimization (global and separate) are also similar, even though some differences are visible at a few temperatures. Since the complex modulus is estimated directly from the optimization of the FRFs, the phase angle can be determined without any additional methods.

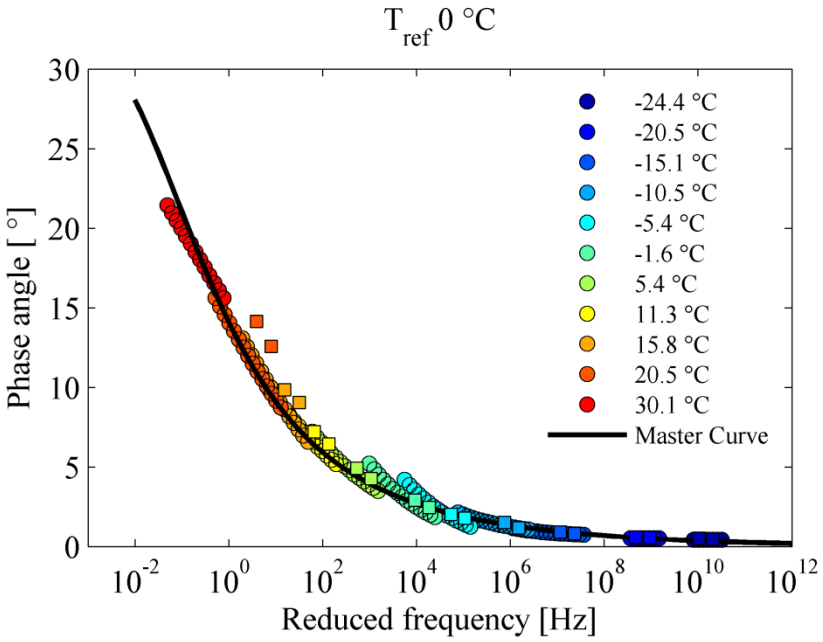

Fig. 8 The phase angle determined by RAS – □, separate optimization of the FRFs – ○ and global optimization of the FRFs (master curve).

The Cole-Cole diagram presented in figure 9 acts as an indication of the accuracy of the estimated master curve due to that it is independent of any shift factors and presenting the loss modulus against the storage modulus. Therefore, a unique curve is expected for the complex moduli determined for each temperature separately. If not a unique curve is obtained the assumption of a thermorheological simple behavior of the material may not be true, leading to that a master curve cannot be determined. The match between the complex moduli determined through the separate FRF optimization and the global FRF optimization is fairly good, showing that the use of FRFs is a promising approach to determine master curves of asphalt concrete specimens. However, the difference of the complex moduli results of RAS and FRFs are much more obvious in this figure. This difference that has been seen through all of these figures is believed to be caused by limited accuracy of the half-power bandwidth method. Other research has also shown that the accuracy of this method decreases as the damping increases (Wang 2011).

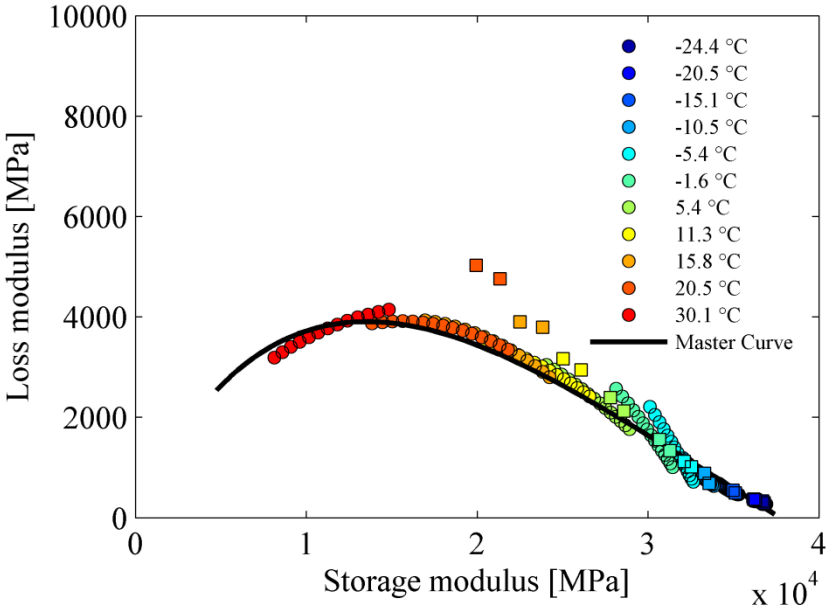

Fig. 9 Cole-Cole diagram of the complex moduli determined by RAS – □, separate optimization of the FRFs – ○ and global optimization of the FRFs (master curve).

The results presented in this chapter and in the appended papers have not been compared to any results obtained from conventional standard testing of the complex modulus. This is partly because this comparison has been considered to be beyond the scope of this thesis, but also because of the different magnitude of the strain levels subjected to the specimens in the different tests. Results obtained from seismic testing (low strain levels) and conventional test methods (higher strain levels) are not expected to be same due the strain level dependency of asphalt concrete. Therefore, the Cole-Cole diagram has been used alone as an indication of the accuracy of the estimated master curve. Furthermore, the applied approaches (ASTM E 1876-99, RAS and FRFs) of estimating the repeatable seismic measurements have given very similar results of the dynamic modulus. This serves as a good indication of the accuracy of the results obtained through seismic testing.

5. Summary of findings

Laboratory seismic measurements have proven to be able to characterize the complex modulus of asphalt concrete over a wide frequency range. The conventional standard laboratory test methods have several disadvantages as high cost, relatively low accuracy and time consuming test procedures. The traditional methods are also limited to testing of the complex modulus within a narrow frequency range. In contrast, the seismic measurements are fast and simple to perform, cost efficient and have a high repeatability and reproducibility. Some disadvantages using seismic testing are that it may not be possible to characterize the material properties at as low frequencies as the conventional testing. The measurements are also performed at a much lower strain level than what an actual pavement are exposed to.

The use of FRFs gives several advantages compared to other methods for seismic evaluation of the complex modulus. The ultrasonic testing provides complex moduli above 20 kHz, the ASTM C215 standard limits the complex modulus to the fundamental resonance frequency and RAS suffers from the need of mode identification and that it must be combined with a method to estimate the intrinsic damping of the material. Importantly, the optimization of FRFs can characterize the complex moduli over a wider frequency range than the other presented methods, which opens up the possibility to determine master curves. A disadvantage with the proposed FRF method is that relatively heavy computer simulation is needed, which increases the time taken to analyze the seismic measurements. However, the theoretical calculation of the FRFs holds the potential for further development by using analytical calculations or by improving the current numerical calculations.

The comparison between RAS and the FRF optimization method show that the optimization of FRFs gives more accurate results due to an improved estimation of the damping. Furthermore, the FRF method can provide a good estimation of the complex modulus master curve of an asphalt concrete specimen.

Seismic measurements provide a truly nondestructive alternative to characterize material properties of asphalt concrete in both laboratory and field. Therefore, seismic measurements can be an efficient technique to improve the knowledge of the quality of roads by better quality controls and quality assurance of pavement structures. This can lead to improved production and maintenance of pavements. Finally, laboratory seismic testing opens up the possibility of performing highly detailed measurements of asphalt concrete that can give new insights and knowledge of the material.

6. References

ASTM (**2008**), C215-08, *Standard Test Method for Fundamental Transverse, Longitudinal, and Torsional Frequencies of Concrete Specimens* (American Society for Testing and Materials, West Conshohocken, PA)

ASTM (**1999**), E 1876-99, *Standard test method for dynamic Young's modulus, shear modulus, and Poisson's ratio by impulse excitation of vibration* (American Society for Testing and Materials, West Conshohocken, PA).

Brown, E. R., Kandhal, P. S., Roberts, F. L., Kim, Y. R., Lee, D. Y., Kennedy, T. W. (**2009**). *Hot Mix Asphalt Materials, Mixture Design and Construction* (NAPA Research and Education Foundation, Lanham, MD)

Demarest, H. H. (**1971**) "Cube-resonance method to determine the elastic constants of solids", J. Acoust. Soc. Am. **49**, 768-775.

Di Benedetto, H., Sauzéat, C., Sohm, J. (**2009**) "Stiffness of Bituminous Mixtures Using Ultrasonic Wave Propagation", Road Mater. Pavement Des. **10**(4), 789-814.

Guo, Q., Brown, D. A. (**2000**) "Determination of the dynamic elastic moduli and internal friction using thin resonant bars", J. Acoust. Soc. Am. **108**(1), 167-174.

Holland, R. (**1968**) "Resonant properties of piezoelectric ceramic rectangular parallelepipeds", J. Acoust. Soc. Am. **43**, 988-997.

Kim, Y. R., Seo, Y., King, M., Momen, M. (**2004**). "Dynamic Modulus Testing of Asphalt Concrete in Indirect Tension Mode", J. Transp. Res. Board **1891**, 163-173.

Kweon, G., and Kim, Y. R. (**2006**). "Determination of the complex modulus of asphalt concrete using the impact resonance test", J. Transp. Res. Board **1970**, 151–160.

Lacroix, A., Kim, Y. R., and Far, M. S. S. (**2009**). "Constructing the dynamic modulus mastercurve using impact resonance testing", Assoc. Asph. Paving Technol. **78**, 67–102.

Leisure, R. G., Willis, F. A. (**1997**). "Resonant Ultrasound Spectroscopy" J. Phys.: Condens. Matter **9**, 6001-6029.

Li, G., Gladden, J.R. (**2010**) "High Temperature Resonant Ultrasound Spectroscopy: A Review", Int. J. Spectroscopy doi:10.1155/2010/206362.

Migliori, A., Sarrao, J. L. (**1997**). *Resonant Ultrasound Spectroscopy – Applications to Physics, Materials Measurements and Nondestructive Evaluation* (Wiley – Interscience Publication, New York)

Migliori, A., Sarrao, J. L., Visscher, W. M., Bell, T. M., Lei, M., Fisk, Z., Leisure, R.G. (**1993**) " Resonant ultrasound spectroscopic techniques for measurement of the elastic moduli of solids", Physica B **183**, 1-24.

Nazarian, S., Desai, M. R. (**1993**). “Automated Surface Wave Method: Field Testing”, J. Geotech. Engrg. ASCE **119**(7), 1094-1111.

Nazarian, S., Tandon, V., Yuan, D. (**2005**). “Mechanistic Quality Management of Hot Mix Asphalt Layers with Seismic Methods”, J. ASTM Int. **2**(9).

Nazarian, S., Yuan, D., Tandon, V. (**1999**). “Structural Field Testing of Flexible Pavement Layers with Seismic Methods for Quality Control” J. Transp. Res. Board **1654**, 50-60.

Norambuena-Contreras, J., Catsro-Fresno, D., Vega-Zamanillo, A., Celaya, M., Lombillo-Vozmediano, I., (**2010**) “Dynamic modulus of asphalt mixture by ultrasonic direct test”, NDT&E Int. **43**, 629-634.

Ohno, I. (**1976**) “Free vibration of a rectangular parallelepiped crystal and its application to determination of elastic constants of orthorhombic crystals”, J. Phys. Earth **24**(4), 355-379.

Ostrovsky, L., Lebedev, A., Matveyev, A., Potapov, A., Sutin, A., Soustova, I., Johnson, P. (**2001**). "Application of three-dimensional resonant acoustic spectroscopy method to rock and building materials", J. Acoust. Soc. Am. **110**(4), 1770-1777.

Popovics, J. S., Rose, J. L. (**1994**). “A Survey of Developments in Ultrasonic NDE of Concrete”, IEEE Transactions on Ultrasonics, Ferroelectrics, and Frequency Control **41**(1), 140-143.

Ren, Z., Atalla, N., Ghinet, S. (**2011**) “Optimization Based Identification of the Dynamic Properties of Linearly Viscoelastic Materials Using Vibrating Beam Technique”, ASME J. Vib. Acoust. **133**(4), 041012 1-12.

Renault, A., Jaouen, L., Sgard, F. (**2011**) “Characterization of elastic parameters of acoustical porous materials from beam bending vibrations”, J. Sound Vib. **330**, 1950-1963.

Rupitsch, S. J., Ilg, J., Sutor, A., Lerch, R., Döllinger, M. (2011) “Simulation based estimation of dynamic mechanical properties for viscoelatic materials used for vocal fold models”, J. Sound Vib. **330**, 4447-4459.

Ryden, N. (**2004**) “Surface wave testing of pavements”, Doctoral thesis, Lund Institute of Technology, Lund University, ISBN 91-973406-4-2.

TRVK Väg (**2011**), *Trafikverkets tekniska krav Vägbyggnad*, Tomas Winnerholt, Trafikverket, Borlänge, ISBN: 978-91-7467-137-7.

Visscher, W. M., Migliori, A., Bell, T. M., Reinert, R. A. (**1991**) “On the normal modes of free vibration of inhomogeneous and anisotropic elastic objects”, J. Acoust. Soc. Am. **90**(4), 2154-2162.

Wang, I. (**2011**) “An Analysis of Higher Order Effects in the Half Power Method for Calculating Damping”, *J. Appl. Mech.* **78**, 014501.

Wang, J.- T., Jin, F., Zhang, C.- H. (**2012**) “Estimation error of the half-power bandwidth method in identifying damping for multi-DOF systems”, *Soil Dyn. Earthquake Eng.* **39**, 138-142.

Whitmoyer, S. L., and Kim, Y. R. (**1994**). “Determining asphalt concrete properties via the impact resonant method”, J. Test. Eval. **22**(2), 139–148.

Williams, M. L., Landel, R. F., Ferry, J. D. (**1955**) “The temperature dependence of relaxation mechanisms in amorphous polymers and other glass-forming liquids”, J. Am. Chem. Soc. **77**, 3701.

Paper I

Gudmarsson, A., Ryden, N., Birgisson, B., 2012, Application of resonant acoustic spectroscopy to asphalt concrete beams for determination of the dynamic modulus, Materials and Structures, DOI: 10.1617/s11527-012-9877-3.

Materials and Structures
DOI 10.1617/s11527-012-9877-3

ORIGINAL ARTICLE

Application of resonant acoustic spectroscopy to asphalt concrete beams for determination of the dynamic modulus

A. Gudmarsson · N. Ryden · B. Birgisson

Received: 11 April 2011 / Accepted: 21 May 2012

Abstract In this paper, a new application of resonant acoustic spectroscopy (RAS) is examined for constructing asphalt concrete mastercurves from seismic testing. The frequency-dependent material properties can be characterized from multiple modes of vibration through the use of RAS. Beam-shaped asphalt specimens are tested at multiple temperatures to determine the resonance frequencies of the specimens. The resonance frequencies are estimated by applying a small load impulse and measuring the resulting acceleration through the specimens. Using RAS, the material properties of the specimens are determined numerically using the measured resonance frequencies. The results presented show that the frequency-dependent dynamic modulus of the asphalt concrete specimens can be characterized using several modes of vibration at each testing temperature.

Keywords Resonant acoustic spectroscopy · Resonance frequency · Dynamic modulus · Mastercurve

A. Gudmarsson (✉) · B. Birgisson
Highway and Railway Engineering, Royal Institute of Technology, Brinellvägen 23, 100 44 Stockholm, Sweden
e-mail: anders.gudmarsson@abe.kth.se

N. Ryden
Engineering Geology, Faculty of Engineering, Lund University, Box 118, 221 00 Lund, Sweden

Published online: 15 June 2012

1 Introduction

The dynamic modulus mastercurve describes the material behavior as a function of temperature and frequency and is therefore a key parameter in modern pavement design and management. Traditional methods to determine the dynamic modulus mastercurve for asphalt concrete are based on cyclic loading over a range of frequencies (0.1–25 Hz) at different temperatures [1]. These tests are time consuming and require expensive equipment and are therefore inappropriate for control during construction. It is also important that the testing is truly non-destructive so that the properties of the specimen do not change during the test.

Resonance frequencies depend on the geometry, mass, boundary conditions and the material properties of a solid and can therefore be used to calculate the dynamic modulus. Measurements based on exciting the resonance frequencies of elastic or viscoelastic objects to determine the material properties are widely known as resonant ultrasound spectroscopy (RUS). Within the civil engineering field the method is also known as free–free resonant column test or impact resonance test. However, it should be noted that traditional RUS is usually based on multiple modes of vibration while applications in civil engineering have so far mostly been restricted to the fundamental modes of vibration.

Previous papers reporting the use of seismic testing applied to asphalt concrete specimens have been based on wave propagation techniques [6, 9], free–free

resonant column test [16] and ultrasonic direct test [17]. The material properties presented in these papers have all been determined from the fundamental modes of vibration. In RUS, unlike in the other methods, the evaluation of the data is always based on numerical methods to obtain the elastic properties of the material, since a complete analytical solution of the problem does not exist today. In fact the efficient and accurate calculation of resonance frequencies of a solid is a central requirement for the application of RUS [15]. Since the development of computer data processing, the use of RUS within different applications has been increasing and it is now a well-established method in many fields for determination of material properties [12, 18].

For measurements that are not only in the ultrasound frequency range (>20 kHz), it has been suggested that the method should be called resonant acoustic spectroscopy (RAS) [18]. Since material properties of asphalt concrete at lower frequencies are of key importance to pavement response analysis, RAS is used in this paper.

Fundamental single mode testing on asphalt concrete has previously been investigated using ASTM C215, which is a standard test method for concrete specimens where the fundamental frequency of the transverse, longitudinal and torsional modes can be determined [2]. A wide range of asphalt mixtures have been tested with the ASTM C215 method and a good agreement with traditional methods has been shown [10, 11, 22]. Limitations with the ASTM standard include that it should only be applied to specimens with a Length (L) to Diameter (D) ratio of $L/D > 2$ and that only the first resonant frequency from each mode type can be used in the evaluation [2]. In order to construct the mastercurve from measurements of the fundamental frequency, shift factors from the binder have been used as representative of the mixture shift factors [11]. Previous research has shown that this assumption is a good approximation [5, 7].

However, RAS based on variational methods, such as the Rayleigh–Ritz algorithm allows for using several frequencies from the same temperature in the evaluation. The damping characteristic of the material forces a limit for how many resonance frequencies can be used in the evaluation. When the damping is too high it will no longer be possible to determine the resonances. In traditional applications of RUS and RAS multiple modes are measured and used in the evaluation of isotropic or anisotropic Young's modulus (E) and Poisson's ratio (υ) to increase the accuracy of the estimated parameters. In the case of a viscoelastic material, multiple modes facilitate the interpretation of the frequency dependent material properties, which is necessary in the construction of a mastercurve directly from RAS [14]. Another important advantage with RAS is that it is applicable to objects of arbitrary geometries [15].

Results from RAS applied to cylindrical disc-shaped asphalt concrete specimens evaluated with the Rayleigh–Ritz method have shown good correlation with mastercurves from the Witczak dynamic modulus predictive model in the high modulus range of the mastercurve [19]. However, the measurements reported were limited to the fundamental flexural mode and the fundamental longitudinal mode. Therefore, there is a need to explore the possibility of using multiple modes of vibration to determine the material properties of asphalt concrete.

The objective of this paper is to investigate the use of RAS applied to beam-shaped asphalt concrete specimens to determine the material properties of asphalt concrete from several flexural and longitudinal resonant modes. This method opens the possibility to determine the high frequency (or low temperature) part of the dynamic modulus mastercurve.

In this paper it is shown that by applying RAS to beam shaped asphalt concrete specimens, the dynamic modulus can be characterized for several resonance modes at each testing temperature.

2 The dynamic modulus mastercurve

The dynamic modulus, $|E^*|$, is the absolute value of the complex modulus, E^*, which is defined as:

$$E^* = E' + iE'' = |E^*|e^{i\phi} \tag{1}$$

where E' is the storage modulus, E'' is the loss modulus and ϕ is the phase angle between those.

In traditional dynamic modulus testing of asphalt concrete, sinusoidal loads are applied to a specimen while measuring its deformation:

$$|E^*| = \frac{\sigma_0}{\varepsilon_0}, \tag{2}$$

where σ_0 is the peak-to-peak stress amplitude and ε_0 is the peak-to-peak strain amplitude.

To consider the temperature and frequency dependence of asphalt concrete, this testing is performed at several different temperatures over a limited frequency range (0.1–25 Hz). Assuming a thermorheologically simple material, these measurements are equivalent to measurements made at a specific temperature over a wider range of frequencies. According to the time–temperature superposition principle, a temperature-dependent shift function is used to shift the test results along the frequency axis to a single mastercurve. The following equations are commonly used in the determination of the mastercurve. Reduced frequencies are calculated to shift the data along the frequency axis,

$$f_{\text{red}} = \alpha_{\text{T}} f \tag{3}$$

where the shift factors, α_{T} can be calculated with the Williams–Landel–Ferry equation [23],

$$\log \alpha_{\text{T}} = \frac{-c_1(T - T_{\text{ref}})}{c_2 + T - T_{\text{ref}}} \tag{4}$$

The coefficients c_1 and c_2 are unknown constants that are estimated along with δ, α, β and γ (the unknown constants in the sigmoidal function),

$$\log|E^*| = \delta + \frac{\alpha}{1 + e^{(\beta - \gamma \log(f_{\text{red}}))}} \tag{5}$$

by fitting the calculated dynamic modulus with the measured dynamic modulus.

3 Resonant acoustic spectroscopy

The computation of the elastic parameters in RUS is based on two parts. First, the so-called forward problem is solved where an approximation of the elastic parameters is made in order to calculate the theoretical natural frequencies. Secondly, the inverse problem is solved where the theoretically calculated natural frequencies are fitted to the measured natural frequencies iteratively, by adjusting the approximated elastic parameters until the best least-square fit is obtained.

Through history, two general approaches have been used to determine resonance frequencies of solids non-analytically. One of the approaches is the finite element method, in which the solid is divided into elements and the governing physical equations for each element are solved separately, under the condition that there is continuity across the element boundaries. The theoretical development of RUS is instead based on the approach of energy minimization techniques that search only for the minimum energy configuration of the body, ensuring that none of the vibrational modes are excluded [15].

The algorithm for calculating the eigenfrequencies of a body has been described in work by Migliori and Sarrao [15]. Here we present only the concept of the energy minimization techniques and how we apply it to beam-shaped asphalt concrete specimens.

From classical mechanics it can be shown that the free vibration of a body is exactly the same as the solution of Lagrangian mechanics for a 3D linear elastic body of arbitrary shape,

$$L = \int_V (KE - PE)\mathrm{d}V, \tag{6}$$

where L is the Lagrangian, KE is the kinetic energy and PE is the potential energy of the body with the volume V. By assuming simple harmonic motion, the equilibrium configuration of the system can be found and the displacements that fulfill this state correspond perfectly to the normal modes of the system. In order to evaluate the displacements numerically, the Rayleigh–Ritz method is used to expand each displacement component (u_i) in terms of basis functions (ϕ_λ):

$$u_i = \sum_\lambda a_{i\lambda}\phi_\lambda, \tag{7}$$

where the coefficients $a_{i\lambda}$ are constants and $\lambda = (p, q, r)$, which are positive integers.

Different types of basis functions for the displacements can be used depending on the geometry of the sample. However, by using powers of Cartesian coordinates a solution can be found for samples with different types of geometry. This is also the chosen basis function in this paper:

$$\phi_\lambda = x^p y^q z^r \tag{8}$$

Now substituting the displacement function into the Lagrangian gives the following matrix equation:

$$L = \frac{1}{2}\omega^2 \vec{a}^T \overleftrightarrow{E}\, \vec{a} - \frac{1}{2}\vec{a}^T \overleftrightarrow{\Gamma}\, \vec{a} \tag{9}$$

where $\overleftrightarrow{E}$ denotes the E matrix, $\overleftrightarrow{\Gamma}$ denotes the Γ matrix, $\vec{a}$ the eigenvectors and ω^2 the eigenvalues.

This matrix equation (Eq. 9) is the complete solution of the system when $N \to \infty$, where N is an

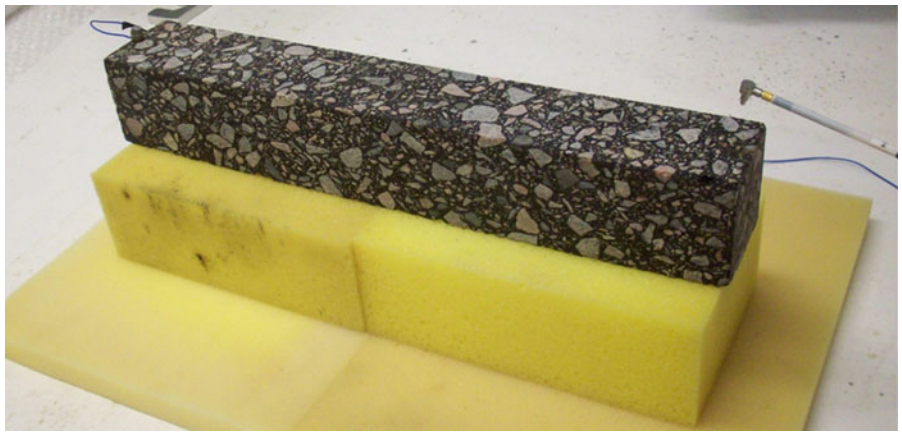

Fig. 1 The test set-up for resonance testing with free boundary conditions

arbitrarily chosen upper limit (usually $N = 10$) to balance the computational time against the number of resonance frequencies needed to determine the elastic parameters with certain accuracy [15]. This is commonly done by:

$$p + q + r \leq N \tag{10}$$

The final eigenvalue equation is obtained considering that the Lagrangian is stationary for the natural frequencies. Therefore the solutions to the problem can be found when the derivatives $\partial L/\partial a_{i\lambda}$ are equal to zero, which gives:

$$\omega^2 \overleftrightarrow{E}\,\vec{a} = \overleftrightarrow{\Gamma}\vec{a} \tag{11}$$

For rectangular parallelepiped samples with the length of the sides of $2d_1$, $2d_2$ and $2d_3$ the calculations of the Γ and E matrices can be reduced by calculating the following analytical formulation [15],

$$f(p,q,r) = \frac{8d_1^{p+1}d_2^{q+1}d_3^{r+1}}{(p+1)(q+1)(r+1)} \tag{12}$$

Now solving the Lagrangian with the Rayleigh–Ritz approximation, the displacements that give the minimum (stationary) solution can be found (from the eigenvectors $\vec{a}$) and the natural frequencies without losses can be determined (from the eigenvalues ω^2).

3.1 Test procedure and analysis

The theory behind RAS requires that the specimen have free boundary conditions. By using pads of soft foam it is assumed that the specimen is floating with free boundary conditions [22]. To excite the normal modes of vibration, a small hammer is used to manually apply a small load impulse to the specimen. An accelerometer (PCB model 352B10) with the weight of 1.5 g, attached to the specimen by wax, is used to transform the resulting vibrations in the specimen into electrical signals. The miniature accelerometer is assumed to have no influence on the resonance frequencies of the beam. Figure 1 presents the set-up used for the resonance testing.

Each 10 ms long signal is stored in a computer by the PC-CARD DAS 16/16-AO from Measurement Computing and by using the Fast Fourier Transform (FFT) the signals are transformed from time domain to frequency domain. Figure 2a shows the measured data in time domain and Fig. 2b the transformed data in frequency domain, where each peak is a resonance mode. Figure 3 illustrates the displacements of the beam for the first three flexural and longitudinal modes.

The test procedure has been repeated for each testing temperature (−10, 0, 10, 20, 25 and 30 °C). At each temperature, three different excitation directions were used to extract as many modes of vibration as possible. For each mode type, ten load impulses were applied to the specimen and the average resonance frequencies from these load impulses were used in the determination of the dynamic modulus. The coefficient of variation for the fundamental resonant frequencies from the ten load impulses was calculated to analyze the repeatability of the measurements. The repeatability is presented in Fig. 4 for the fundamental flexural mode of the different specimens. The good repeatability is a known advantage of resonance

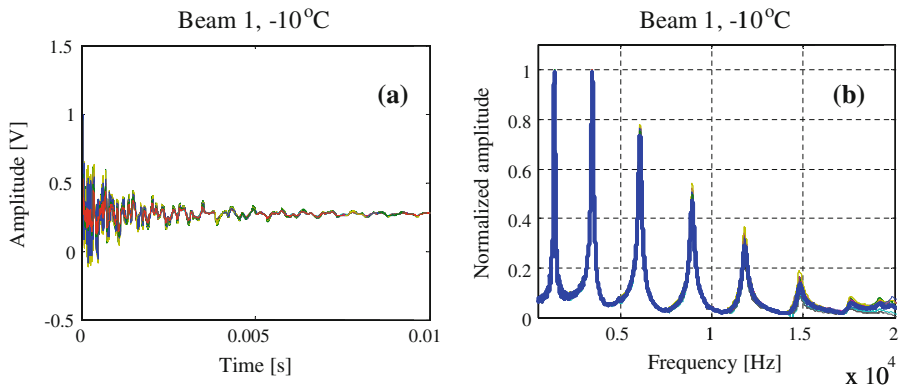

Fig. 2 Data from resonance testing in time domain (**a**) and in frequency domain (**b**)

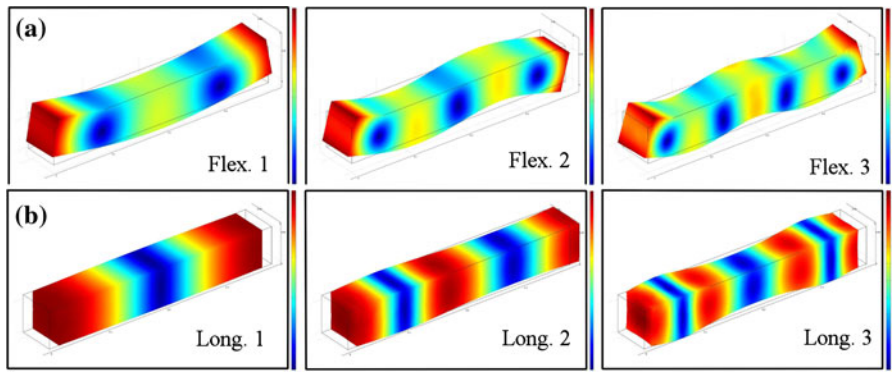

Fig. 3 Illustration of the 3 first flexural modes (**a**) and the 3 first longitudinal modes (**b**)

testing [6, 10, 11, 22]. The three different excitation directions are illustrated in Fig. 5, along with the direction of the beams in the compacted slab.

The measured resonance frequencies from this procedure are the damped natural frequencies of the specimen. These measured resonance frequencies must therefore be converted to natural frequencies before comparison with the theoretically calculated natural frequencies. This is done according to:

$$f_{\mathrm{n}} = \frac{f_{\mathrm{d}}}{\sqrt{1-\zeta^2}} \tag{13}$$

where f_{n} is the natural frequency, f_{d} is the damped natural frequency and ζ is the damping ratio. The damping ratio is determined according to the half-power bandwidth method,

$$\zeta = \frac{\Delta f}{2 f_{\mathrm{d}}} \tag{14}$$

where Δf is the width of the frequency response curve at 0.707 (half-power) of the maximum amplitude of the curve. The damping ratio is also used to determine the phase angle, ϕ,

$$\phi = \arctan(2\zeta) \tag{15}$$

This procedure of estimating damping is applicable as long as the damping ratio does not exceed approximately 0.5 (half of the critical damping) and the recorded length of the signal is longer than the inverse of the bandwidth (Δf) [22].

To find the elastic modulus, knowledge about Poisson's ratio (υ) is needed. At this point Poisson's ratio has been estimated iteratively from the dynamic modulus with the relationship used in the NCHRP Guide for Mechanistic-Empirical Design [8],

$$\upsilon = 0.15 + \frac{0.35}{1 + e^{(a+b\times\log(E))}} \tag{16}$$

To account for the energy losses in the material that have been excluded so far, the phase angle is used to determine the dynamic modulus,

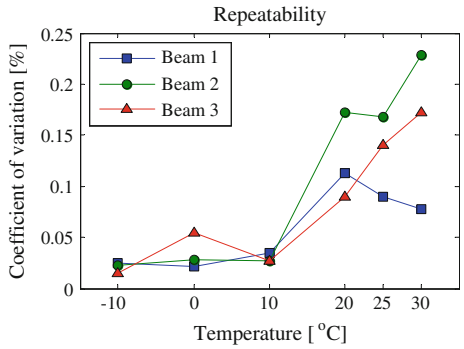

Fig. 4 The repeatability of resonance testing for the fundamental flexural modes in z-direction

$$|E^*| = \frac{E'}{\cos(\phi)} \tag{17}$$

where E' is the storage modulus.

In the application of RUS, it has been suggested that the number of resonance frequencies to accurately fit the elastic parameters should be at least five times the number of unknown parameters to be determined. This requirement has been developed from the experience of the RUS users through history. Due to the viscoelasticity in asphalt concrete each frequency results in different elastic parameters and this requirement can therefore not be fulfilled in this application. Considering that RUS aims to determine a relative accuracy of 10^{-6} and the traditional standards within the pavement industry accepts variations of 10 % this requirement may not be necessary to successfully apply RAS to asphalt concrete [15, 20].

4 Materials

A common mixture used in Swedish pavements, with an accepted range of air voids between 1.5–3.5 % and a minimum binder content of 6.0 % by weight, called ABT 16 70/100 has been tested in this study [21]. Granite aggregates from the Bjärsgård quarry in Skåne with the nominal aggregate size of 16 mm and binder with penetration grade 70/100 from Nynas AB were used in the mixture. The mixing of the asphalt concrete was made in a laboratory mixer with an electrical heating function and a thermometer monitoring the mixing temperature. The mixture was compacted into a slab with the dimensions of 500*560*80 mm (x, y, z) in a laboratory with a roller (see Fig. 5). From the slab, rectangular parallelepiped specimens were sawn along all sides. The positions of the beams related to the slab are presented in Fig. 6 and the dimensions of the three beams are presented in Table 1. Using RAS

Table 1 Specimen data

	Beam 1	Beam 2	Beam 3
Width (y-dir.) (mm)	58.74	58.74	58.65
Height (z-dir.) (mm)	58.87	58.94	58.88
Length (x-dir.) (mm)	382.0	382.0	382.0
Mass (g)	3133	3120	3126
Density (g/cm^3)	2.372	2.359	2.370
Air voids (%)	2.2	2.7	2.3

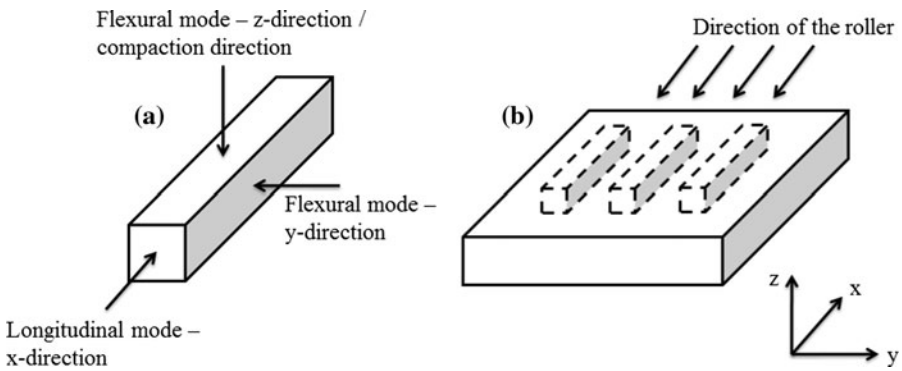

Fig. 5 Measured modes of vibrations (**a**) and the direction of the beams in the slab (**b**)

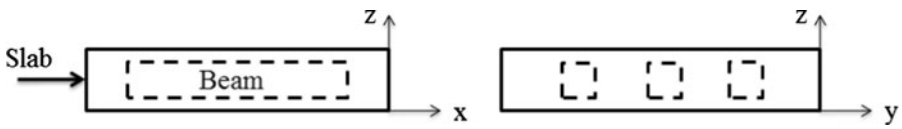

Fig. 6 The cut out beams position in the compacted slab

Table 2 Gradation of the mix

Sieve size (mm)	0.063	0.125	0.25	0.5	1	2	4	5.6	8	11.2	16	22.4
Passing (%)	8.9	12	16	21	28	39	50	58	70	81	98	100
Upper limit (%)	9	–	–	30	–	47	–	–	73	88	100	100
Lower limit (%)	6	–	–	13	–	26	–	–	57	71	90	100

the measured dimensions are equally important as the measured resonance frequencies.

These dimensions were chosen according to the test standard SS-EN 12697-26:2004, where it is stated that the width and the height should be at least three times the maximum grain size. The length should also be six times the highest value of the height or the width [20]. The temperature during mixing and compaction of the mixture was 150 °C. Table 2 presents the gradation of the mix and the gradation limits. The binder content of the mix was determined to 6.3 % by weight.

A temperature chamber was used for the temperature conditioning of the specimens during the test. The actual temperature of the specimens was controlled using a separate "dummy" specimen with thermometers attached to the center and the edge of the specimen. The test was performed during less than half a minute outside the temperature chamber applying 10 impacts on three different sides of the specimen.

5 Results and discussion

In this paper RAS is compared with the test method, ASTM E 1876-99 Standard test method for dynamic Young's modulus, shear modulus, and Poisson's ratio by impulse excitation of vibration. With ASTM E 1876-99 it is possible to determine the fundamental resonant frequency of each type of vibrational mode by exciting the resonance frequencies from a single impulse. The material is assumed to be elastic, homogeneous and isotropic [3].

The dynamic modulus has been characterized for three resonance frequencies for each type of vibration at the testing temperatures between −10 to 10 °C by using RAS. At the higher temperatures (20 °C to 30 °C), increased damping has limited the number of available resonance frequencies for successful characterization of the dynamic modulus. At this point it was not possible to evaluate the longitudinal modes at 30 °C.

Figures 7, 8 and 9 present the dynamic modulus for each type of vibration calculated from the ASTM E 1876-99 standard and from RAS. The results are presented as an average of the three different samples (Beam 1 to Beam 3). The highest coefficient of variation for the dynamic modulus between the different specimens (over the tested temperature interval) is 4.5- %, 5.3 % and 2.0 % for the flexural modes in *z*-direction, flexural modes in *y*-direction and the longitudinal modes (*x*-direction) respectively.

In the comparison between the two methods (RAS and ASTM E 1876-99) a mastercurve is presented for each method. As seen in Figs. 7, 8 and 9, the evaluated data was not enough to create an overlap of the dynamic modulus between the testing temperatures, which is necessary in order to apply the time–temperature superposition. Binder shift factors have therefore been used to construct the mastercurve. The binder shift factors presented in Table 3 have been determined from frequency sweep dynamic shear rheometer measurements.

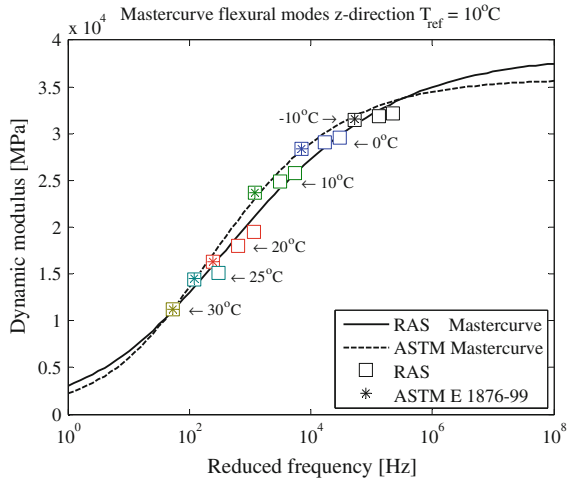

Fig. 7 The average dynamic modulus mastercurve of Beams 1–3 for the flexural modes in the *z*-direction calculated from both the ASTM E 1876-99 standard and RAS. The mastercurves are constructed from binder shift factors

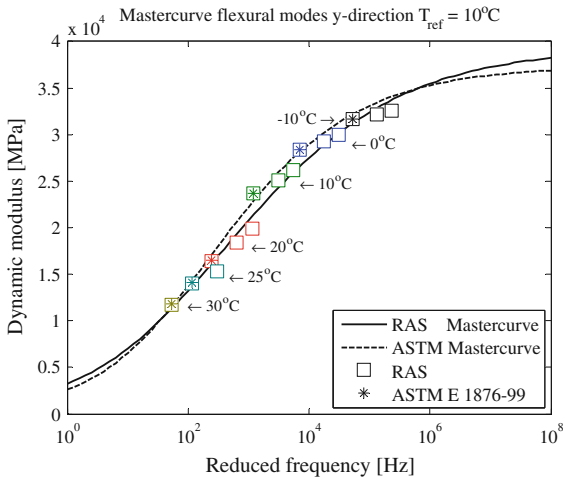

Fig. 8 The average dynamic modulus mastercurve of Beams 1–3 for the flexural modes in the *y*-direction calculated from both the ASTM E 1876-99 standard and RAS. The mastercurves are constructed from binder shift factors

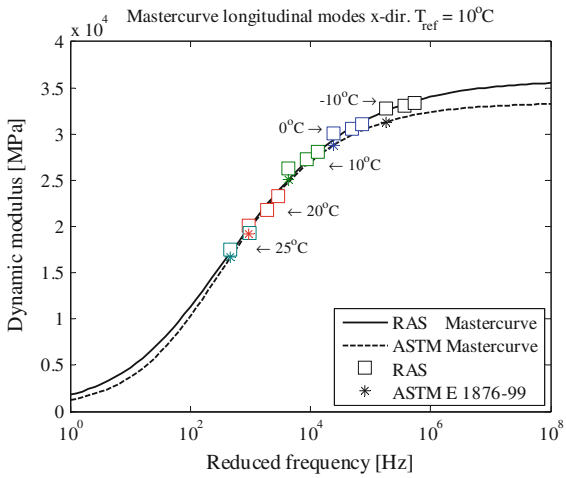

Fig. 9 The average dynamic modulus mastercurve of Beams 1–3 for the longitudinal modes (*x*-direction) calculated from both the ASTM E 1876-99 standard and RAS. The mastercurves are constructed from binder shift factors

It can be seen that there is a perfect match between the two methods for the fundamental flexural modes (Figs. 7, 8). However, the match for the fundamental longitudinal mode is not as precise (Fig. 9). This

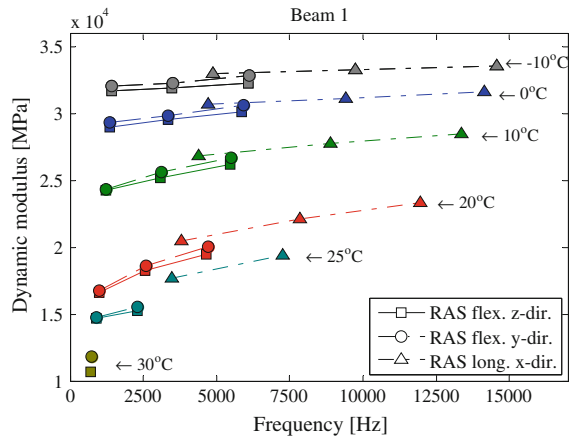

Fig. 10 The dynamic modulus of Beam 1 for the different modes of vibration at the testing temperatures −10, 0, 10, 20, 25 and 30 °C

indicates that for the longitudinal modes of vibration the approximate formulation in the standard test method does not provide precise results for the geometry investigated in this paper. It can also be seen that the shape of the mastercurves differs between the two methods for all mode types (Figs. 7, 8, 9). This fact highlights the importance of characterizing the dynamic modulus using multiple modes of vibration.

Looking more closely to the evaluated dynamic modulus from RAS for the different beams, it can be seen in Figs. 10, 11 and 12 that there is a systematic difference in the dynamic modulus for the different mode types. The most noticeable difference is between the flexural modes of vibration and the longitudinal modes of vibration, where the longitudinal mode type has higher dynamic modulus especially at high temperatures. However, there is also a small difference in the dynamic modulus between the flexural modes in *z*-direction and the flexural modes in the *y*-direction. Here the *y*-direction in general has a slightly higher dynamic modulus than the *z*-direction.

These specific results of the anisotropy, where the modulus is higher in the *y*-direction than in the *z*-direction, have also been seen by Di Benedetto et al. [6] for rolling wheel compacted asphalt concrete. One reason for this could be that the aggregates tend to

Table 3 Binder shift factors

Temperature (°C)	−10	0	10	20	25	30
Log(α_T)	1.5733	0.7163	0	−0.6077	−0.8782	−1.1296

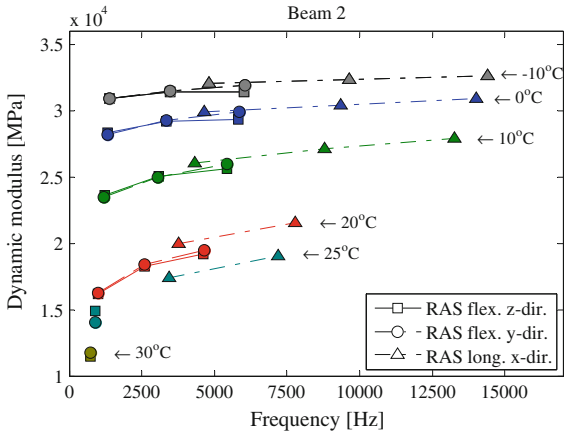

Fig. 11 The dynamic modulus of Beam 2 for the different modes of vibration at the testing temperatures −10, 0, 10, 20, 25 and 30 °C

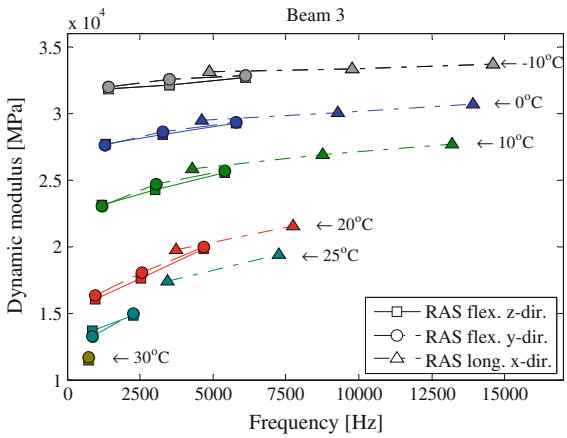

Fig. 12 The dynamic modulus of Beam 3 for the different modes of vibration at the testing temperatures −10, 0, 10, 20, 25 and 30 °C

orient themselves with the longest axis horizontally during this type of compaction, leading to a stiffer response in the horizontal direction (*y*-direction). These results agree with research showing that the stiffness in the direction of the longest axis is significantly higher than the stiffness in the direction of the aggregates short axis [4]. It can also be seen that the longitudinal horizontal direction gives a higher modulus than both of the flexural mode types. In previous research it has been seen that a stiffening effect is observed when asphalt concrete is subjected to compression [13]. These results of the anisotropy are systematic for the tested specimens and agree well

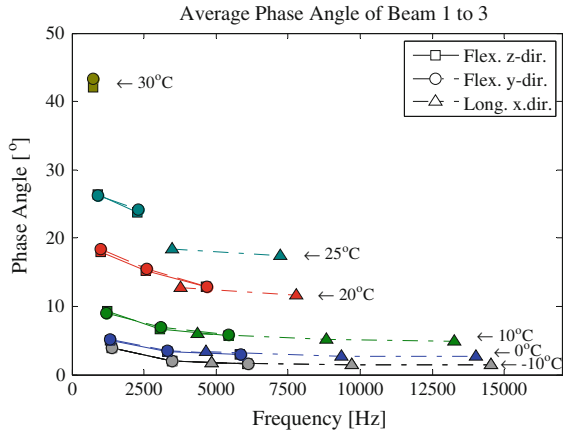

Fig. 13 The measured average phase angle of Beams 1–3 at the testing temperatures −10, 0, 10, 20, 25 and 30 °C

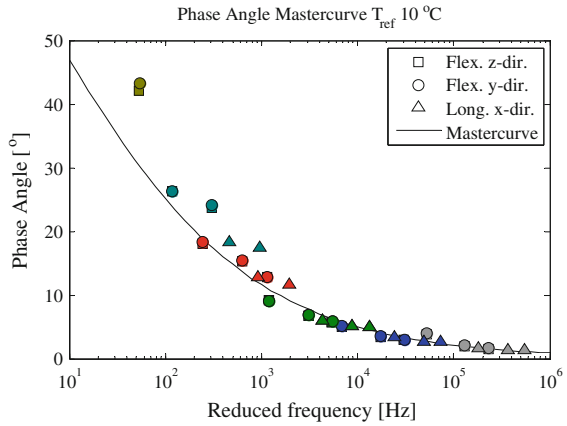

Fig. 14 The measured average phase angle mastercurve

with previous research of anisotropy in asphalt concrete.

Figure 13 shows the result of the measured phase angle as an average of Beam 1 to 3. Using resonance testing, no correction are needed for obtaining the phase angle.

The average phase angle is also presented as a mastercurve in Fig. 14, where the mastercurve was determined from the fitted storage and loss modulus and by using the binder shift factors.

The influence of the air voids on the dynamic modulus is presented in Fig. 15. The specimen with the highest air voids (Beam 2) has the lowest dynamic modulus at 10 kHz and 10 °C. The dynamic modulus at this specific frequency and temperature are calculated from the RAS mastercurve.

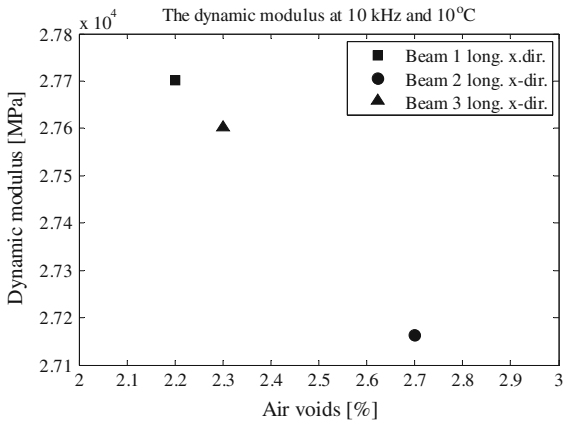

Fig. 15 The dynamic modulus dependency of the air voids at 10 kHz and 10 °C

Table 4 The dynamic modulus at 10 kHz and 10 °C

	Beam 1	Beam 2	Beam 3
Air voids (%)	2.2	2.7	2.3
Flex. *z*-dir. (MPa)	27,539	27,057	27,156
Flex. *y*-dir. (MPa)	27,957	27,249	27,540
Long. *x*-dir. (MPa)	27,702	27,163	27,603

Table 4 presents the dynamic modulus at 10 kHz and 10 °C for the three different mode types. It can be seen that the results in Fig. 15 are typical for all mode types. Also here the dynamic modulus is calculated from the RAS mastercurve.

The coefficients in the equation of Poisson's ratio (Eq. 16) were chosen so that the dynamic modulus increases with increasing mode number (frequency). Figure 16 presents the dynamic modulus dependency of mode number and Poisson's ratio at −10 °C. As shown in Fig. 16 the expected increase in the dynamic modulus with frequency requires a Poisson's ratio above approximately 0.2 at this temperature. The coefficients in Eq. 16 were set to $a = -19$ and $b = 2.95$ based on these results.

The approximation of Poisson's ratio is an uncertainty, but to the authors knowledge there is no other relationship that is known to be more correct in order to describe the frequency dependency of Poisson's ratio. The empirical relation in Eq. 16 is here treated as a first approximation to be further evaluated in future studies using RAS.

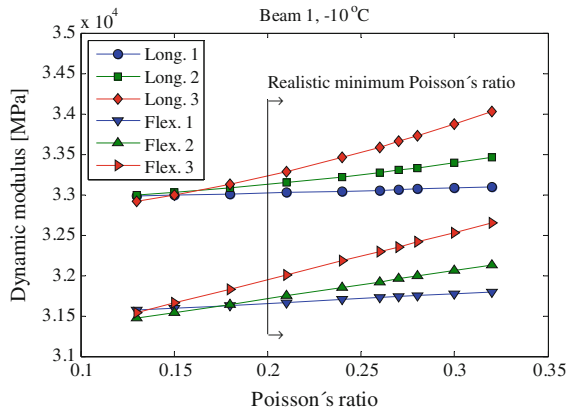

Fig. 16 The dynamic modulus dependency of Poisson's ratio for different modes of vibration

6 Conclusions

The application of RAS to asphalt concrete beams has been investigated in this paper. The results show that the material properties can be characterized for multiple modes of vibration at each testing temperature. Therefore, the dynamic modulus can be characterized for a wider frequency range by using RAS compared to the traditional methods. Since the standard test methods used today to determine the dynamic modulus are limited to testing at maximum 25 Hz (AASHTO 2007), RAS holds the promise of being able to provide more knowledge about asphalt concrete at low temperatures and higher stiffness. The results were also compared to the ASTM E 1876-99 method. The comparison indicated that the approximate formulation (ASTM E 1876-99) for the longitudinal modes of vibration did not provide precise results for the geometry investigated in this paper. The results throughout this paper show a good repeatability of the method.

Importantly, RAS can be used for testing over extended frequency ranges, thus providing increased accuracy in future comparisons with other standard test methods for the dynamic modulus. This knowledge can be used to develop even more accurate and precise theoretical models for asphalt concrete.

Acknowledgments The authors would like to thank the Swedish Transport Administration (Trafikverket) and the Swedish construction industry's organization (SBUF) for their financial support. A great appreciation is also given to Olof Åkesson and Viktor Pettersson at Peab Asfalt's laboratory in Helsingborg for their support in producing and testing the specimens.

References

1. American Association of State Highway and Transportation Officials (AASHTO) (2007) Standard method of test for determining dynamic modulus of hot-mix asphalt mixtures. AASHTO Designation: TP 62, Washington
2. ASTM C215-08 Standard Test Method for Fundamental transverse, longitudinal, and torsional frequencies of concrete specimens. American Society for Testing and Materials (ASTM), New York
3. ASTM E 1876-99, Standard test method for dynamic Young's modulus, shear modulus, and Poisson's ratio by impulse excitation of vibration. American Society for Testing and Materials (ASTM), New York
4. Chen J, Pan T, Huang X (2011) Numerical investigation into the stiffness anisotropy of asphalt concrete from a microstructural perspective. Constr Build Mater. doi:10.1016/j.conbuildmat.2011.01.002
5. Di Benedetto H, Des Croix P (1996) Binder-mix rheology: limits of linear domain, non linear behavior. In: Eurasphalt & Eurobitume congress, Strasbourg, 7–10 May 1996
6. Di Benedetto H, Sauzéat C, Sohm J (2009) Stiffness of bituminous mixtures using ultrasonic wave propagation. Road Mater Pavement Des 10(4):789–814
7. Dongre R, Myers L, D'Angelo J, Paugh C, Gudimettla J (2005) Field evaluation of Witczak and Hirsch models for predicting dynamic modulus of hot–mix asphalt, vol 74, pp 381–442. Association of Asphalt Paving Technologists, Long Beach
8. NCHRP Guide for Mechanistic-Empirical Design (2004) Final Report, Part 2. Design inputs, chap 2. Material Characterization, NCHRP, March 2004
9. Hochuli AS, Sayir MB, Poulikakos LD, Partl MN (2001) Measuring the complex modulus of asphalt mixtures by structural wave propagation. Association of Asphalt Paving Technologists (AAPT), Clearwater Beach, 19–21 March 2001
10. Kweon G, Kim YR (2006) Determination of the complex modulus of asphalt concrete using the impact resonance test. J Transp Res Board 1970:151–160
11. Lacroix A, Kim YR, Far MSS (2009) Constructing the dynamic modulus mastercurve using impact resonance testing. Association of Asphalt Paving Technologists (AAPT)
12. Lebedev AV, Ostrovskiĭ LA, Sutin AM, Soustova IA, Johnson PA (2003) Resonant acoustic spectroscopy at low Q factors. Acoust Phys 49(1):81–87
13. Levenberg E (2006) Constitutive Modeling of asphalt-aggregate mixes with damage and healing. PhD dissertation, Technion, Israel Institute of Technology
14. Madigosky WM, Lee GF (1979) Automated dynamic Young's modulus and loss factor measurements. Naval Surface weapons Center, White Oak, Silver Spring
15. Migliori A, Sarrao JL (1997) Resonant ultrasound spectroscopy—applications to physics, materials measurements and nondestructive evaluation. Wiley-Interscience, New York, ISBN 0-471-12360-9
16. Nazarian S, Yuan D, Tandon V, Arellano M (2005) Quality management of flexible pavement layers with seismic methods. Center for Transportation Infrastructure Systems, Research Report 0-1735-3, The University of Texas at El Paso
17. Norambuena-Contreras J, Catsro-Fresno D, Vega-Zamanillo A, Celaya M, Lombillo-Vozmediano I (2010) Dynamic modulus of asphalt mixture by ultrasonic direct test. NDT&E Int 43:629–634
18. Ostrovsky L, Lebedev A, Matveyev A, Potapov A, Sutin A, Soustova I, Johnson P (2001) Application of three-dimensional resonant acoustic spectroscopy method to rock and building materials. Acoust Soc Am 110:1770–1777
19. Ryden N (2011) Resonant frequency testing of cylindrical asphalt samples. Eur J Environ Civ Eng 15:587–600
20. SS-EN 12697-26:2004, Bituminous mixtures—test methods for hot mix asphalt—part 26: Stiffness, ICS 93.080.20
21. VVTBT (2009) Bitumenbundna lager 09, Publikation 2009:140, Vägverket
22. Whitmoyer SL, Kim YR (1994) Determining asphalt concrete properties via the impact resonant method. J Test Eval 22(2):139–148
23. Williams ML, Landel RF, Ferry JD (1955) The temperature dependence of relaxation mechanisms in amorphous polymers and other glass-forming liquids. J Am Chem Soc 77:3701–3707

Paper II

Gudmarsson, A., Ryden, N., Birgisson, B., 2012, Characterizing the low strain complex modulus of asphalt concrete specimens through optimization of frequency response functions, Journal of Acoustical Society of America, Vol. 132, Issue 4, pp. 2304-2312.

Characterizing the low strain complex modulus of asphalt concrete specimens through optimization of frequency response functions

Anders Gudmarsson,[a] Nils Ryden, and Björn Birgisson
Highway and Railway Engineering, KTH Royal Institute of Technology, Brinellvägen 23, 100 44 Stockholm, Sweden

(Received 18 May 2012; revised 12 July 2012; accepted 1 August 2012)

Measured and finite element simulated frequency response functions are used to characterize the low strain ($\sim 10^{-7}$) complex moduli of an asphalt concrete specimen. The frequency response functions of the specimen are measured at different temperatures by using an instrumented hammer to apply a load and an accelerometer to measure the dynamic response. Theoretical frequency response functions are determined by modeling the specimen as a three-dimensional (3D) linear isotropic viscoelastic material in a finite element program. The complex moduli are characterized by optimizing the theoretical frequency response functions against the measured ones. The method is shown to provide a good fit between the frequency response functions, giving an estimation of the complex modulus between minimum 500 Hz and maximum 18|000 Hz depending on the temperature. Furthermore, the optimization method is shown to give a good estimation of the complex modulus master curve.
 [http://dx.doi.org/10.1121/1.4747016]

PACS number(s): 43.40.At, 43.40.Le, 43.60.Pt, 43.40.Cw [DAB] Pages: 2304–2312

I. INTRODUCTION

Non-destructive testing (NDT) is of great importance for future quality control and quality assurance of new and old pavement constructions. NDT offers a fast, economic, and truly non-destructive method of linking low strain measurements of asphalt concrete from field and laboratory together. Using seismic testing, measurements of specimens in the laboratory are performed at approximately the same strain level as seismic measurements in the field. This allows for a direct comparison between the strain level dependent material properties determined in field and laboratory. Today there are three different standard test methods available to measure the dynamic modulus of asphalt concrete specimens (Brown *et al*., 2009). The dynamic modulus can be measured at minimum 0.01 Hz and maximum 25 Hz through these methods. However, there is no non-destructive measurement technique in the field that can be linked to the results from these methods. In addition, the traditional methods require expensive equipment and are not completely non-destructive. They may also be considered as too time consuming to be used in the daily production.

A general problem with NDT applied to asphalt concrete specimens has been to evaluate the complex modulus at several frequencies at each testing temperature. Previous resonance frequency measurements applied to asphalt concrete specimens have for example been based on the ASTM C215 standard (Whitmoyer and Kim, 1994; Kweon and Kim, 2006; Lacroix *et al*., 2009) and resonant ultrasound spectroscopy (RUS) (Ryden, 2011; Gudmarsson *et al*., 2012). The ASTM C215 standard is limited to determination of the complex modulus to the fundamental modes of vibration (ASTM, 2008), while RUS offers a possibility to determine the complex modulus at more than one resonance frequency (Leisure and Willis, 1997; Migliori and Sarrao, 1997). However, using only the resonances of a specimen for a viscoelastic material usually limits the determination of the modulus to a few numbers of frequencies at a specific temperature (Buchanan, 1987). Ryden (2011) applied resonant acoustic spectroscopy (RAS) (Ostrovsky *et al*., 2001) to cylindrical asphalt concrete disks, characterizing the dynamic modulus for two different fundamental modes of vibration at different temperatures. Gudmarsson *et al*. (2012) characterized the dynamic modulus at most three resonance frequencies per temperature by applying RAS to beam shaped asphalt concrete specimens. In common for all these results applying resonance testing to asphalt concrete is the limitation of not being able to construct master curves using only NDT. So far the construction of the master curve has been based on binder shift factors obtained from measurements of the binder in a lower frequency range (Kweon and Kim, 2006; Lacroix *et al*., 2009; Gudmarsson *et al*., 2012). Therefore the number of measurement points (frequency range) from each temperature needs to be increased to be able to determine master curves using only NDT. Also, the applicability of the time-temperature superposition principle to results obtained from high frequency measurements of asphalt mixtures needs to be further investigated.

Through the use of frequency response functions (FRFs), it is possible to characterize the material properties at a wider range of frequencies and not only at the resonances of a specimen (Buchanan, 1987). Therefore the finite element method is applied in this paper to perform frequency response simulations of a beam shaped asphalt concrete specimen to determine the theoretical frequency response.

[a]Author to whom correspondence should be addressed. Electronic mail: andgud@kth.se

TABLE I. Gradation of the mix (Gudmarsson *et al*., 2012).

Sieve size (mm)	0.063	0.125	0.25	0.5	1	2	4	5.6	8	11.2	16	22.4
Passing (%)	8.9	12	16	21	28	39	50	58	70	81	98	100
Upper limit (%)	*9*	-	-	*30*	-	*47*	-	-	*73*	*88*	*100*	*100*
Lower limit (%)	*6*	-	-	*13*	-	*26*	-	-	*57*	*71*	*90*	*100*

Using this approach, the material properties of a specimen can be determined iteratively over a wide frequency range by fitting theoretical FRFs with measured FRFs. Optimization of FRFs for determination of the material properties of specimens is commonly used in other fields of application. For example, Guo and Brown (2000) and Renault *et al*. (2011) matched measured and analytical determined FRFs of frequency dependent materials to characterize their material properties. Ren *et al*. (2011) evaluated seven parameters describing the temperature and frequency dependent material properties by optimizing FRFs of metal polymer sandwich beams. Rupitsch *et al*. (2011) determined the dynamic complex Young's modulus and Poisson's ratio of a viscoelastic material used for vocal fold models through the use of FRFs. Advantages using FRFs compared to only the resonance frequencies are not only the increased usable frequency range. The procedure of matching the measured resonance frequency with the corresponding theoretical resonance frequency is not always straight forward. This is due to the fact that the computation of the theoretical resonance frequencies gives results of resonance frequencies for all modes of vibration of the solid. Therefore the theoretical resonance frequencies that correspond to the measured mode of vibration must be identified. This is generally rather simple for the first two or three resonance frequencies but may be more problematic for higher resonances, where the resonance frequencies of different modes of vibration may be difficult to differentiate.

The aim of this paper is to expand the frequency range and number of measurement points, from which the complex modulus of asphalt concrete specimens can be characterized through NDT. Moreover, the possibility of constructing asphalt concrete master curves through optimization of FRFs is studied.

II. METHODOLOGY

A. Materials

Measurements have been performed to an asphalt concrete beam and to an unplasticized polyvinyl chloride (PVC-U) beam. The PVC-U beam (398.6 mm × 63.66 mm × 50.08 mm) with the density of 1.374 g/cm^3 has been tested to investigate the applicability of the method.

The asphalt concrete specimen has a nominal aggregate size of 16 mm, and the recipe of the mix follows the criteria of an ABT 16 mixture with 70/100 Nynas bitumen and granite aggregates (Trafikverket, 2009). The mixing of the asphalt concrete was performed in a laboratory mixer at 150 °C, giving a binder content of 6.3% and the gradation according to Table I (Gudmarsson *et al*., 2012). The asphalt mix was compacted with a roller in a laboratory to a slab (500, 560, 80 mm), from which the specimen was sawn out to the dimensions of 382 mm × 58.74 mm × 59.94 mm (x, y, z) according to Fig. 1. The density of the measured specimen is 2.359 g/cm^3, and the air void content of the specimen is 2.7%.

B. Experimental determination of the frequency response function

The test setup used for measuring the FRFs of the beam shaped asphalt concrete specimen is illustrated in Fig. 1. The soft foam is assumed to provide free boundary conditions to the specimen (Whitmoyer and Kim, 1994). The measurements can be applied to specimens with arbitrary geometry.

An impact hammer (PCB model 086E80) is used to apply a load impulse, and an accelerometer (PCB model 352B10) is used to measure the response. The accelerometer is attached to the specimen by soft wax. Note that the accelerometer is very light (0.7 g) and is assumed to have no effect on the response of the system. The impact hammer and the accelerometer are connected to a signal conditioner (PCB model 480B21), which is further connected to a data acquisition device (NI USB-6251 M Series) for analog to digital conversion. The Data Acquisition Toolbox in MATLAB has been used to set up the data acquisition device and to perform the measurements. The data collected from this testing are stored in a computer.

The load impulse in time domain of a measurement at −1.6 °C of the asphalt concrete specimen and the fast Fourier estimation the recorded signals are presented in Figs. 2(a) and 2(b), respectively. The sampling frequency was set to 500 kHz when using the NI USB-6251 M Series device. Figure 3(a) shows the response of the measurement in time domain, and Fig. 3(b) shows the fast Fourier transform of the response in frequency domain. The record lengths of the response were chosen depending on the temperature (damping) of the specimen. At this temperature, 0.008 s was chosen.

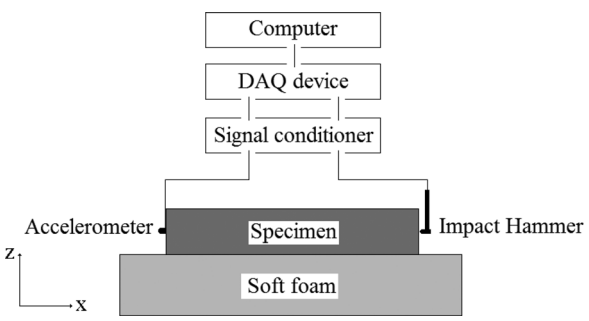

FIG. 1. Illustration of the experimental setup.

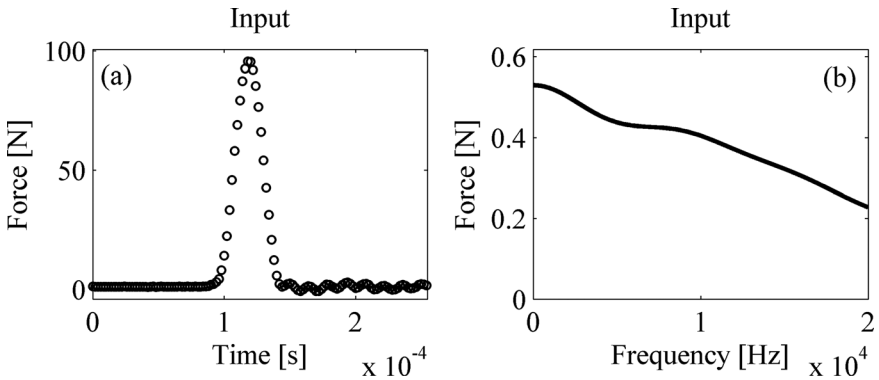

FIG. 2. The load impulse in time domain (a) and frequency domain (b).

A frequency response function (H) can be calculated according to Eq. (1), where Y is the Fourier transform of the measured response (output) and X is the Fourier transform of the load impulse (input),

$$H(f) = \frac{Y(f)}{X(f)}. \tag{1}$$

To reduce measurement noise when determining FRFs, the ratio between the cross power spectrum and the power spectrum [Eq. (2)] is usually used in practice (Halvorsen and Brown, 1977). This equation is also used in this paper to determine the FRFs,

$$H(f) = \frac{X^*(f) \times Y(f)}{X^*(f) \times X(f)}, \tag{2}$$

where $X^*(f)$ = the complex conjugate of $X(f)$.

A FRF of the longitudinal vibration modes (x direction) has been determined for each testing temperature (−24.4 °C, −20.5 °C, −15.1 °C, −10.5 °C, −5.4 °C, −1.6 °C, 5.4 °C, 11.3 °C, 15.8 °C, 20.5, and 30.1 °C). Figure 4(a) presents the absolute value of the measured FRFs for five of the tested temperatures, and Fig. 4(b) presents the unwrapped phase angle of the same temperatures. The FRFs at different temperatures are calculated from an average of five individual measurements at each temperature. The maximum strains applied to the specimen through these tests have been approximated to 0.12 micro-strains. The maximum strains occur at the first resonance frequency and have been approximated by Eq. (3) (Pasqualini, 2006), where ε is the strain, $Y(f)$ is the measured acceleration, L is the length of the specimen, and f is the frequency,

$$\varepsilon = \frac{Y(f)}{4\pi L f^2}. \tag{3}$$

The coherence function presented in Fig. 5 is an indication of the quality of the FRF measurements. A value of zero means no correlation between the impulse signal and the response. A value of one indicates that the response is completely explained by the impulse signal and that there is no other interference. The coherence function is determined from the average of five individual FRF measurements at each temperature. Based on the coherence function, a minimum limit of the usable frequency range to characterize the complex modulus is set to 500 Hz for all temperatures except -20.5 °C and −24.4 °C. At these temperatures, there is some interference up to approximately 4000 Hz, which is set as a minimum limit for these temperatures. The coherence function (CF) is calculated according to Eq. (4),

$$CF = \frac{\left|\left(\overline{X^*(f) \times Y(f)}\right)\right|^2}{\left(\overline{X^*(f) \times X(f)}\right) \times \left(\overline{Y^*(f) \times Y(f)}\right)}, \tag{4}$$

where $\overline{X^*(f) \times Y(f)}$ = averaged cross power spectrum, $\overline{X^*(f) \times X(f)}$ = averaged auto power spectrum (impulse), and $\overline{Y^*(f) \times Y(f)}$ = averaged auto power spectrum (response).

C. Theoretical determination of the frequency response function

The theoretical frequency response analysis of the specimen was performed by using a finite element program (COMSOL MULTIPHYSICS 4.2, 1998), where the specimen was

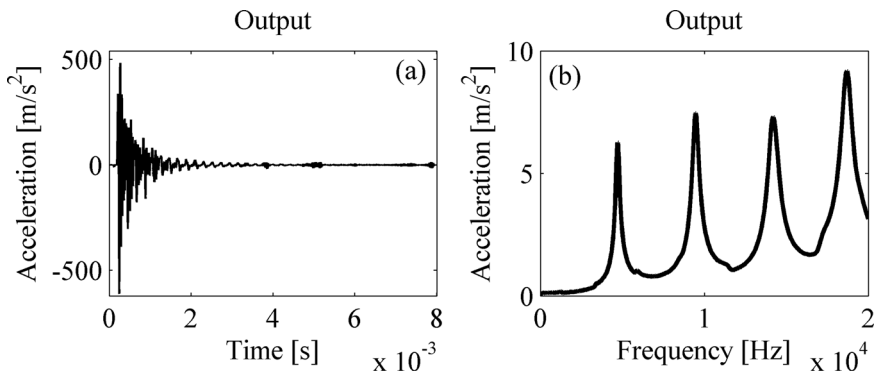

FIG. 3. The measured response of the specimen in time domain (a) and frequency domain (b).

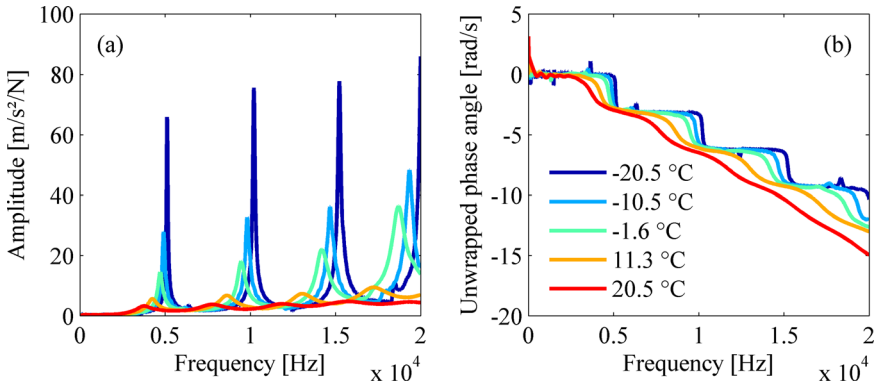

FIG. 4. (Color online) Measured FRFs of the longitudinal vibration modes (a) and the unwrapped phase angle of the measured FRFs (b).

modeled as a 3D linear isotropic viscoelastic material. The viscoelastic parameters of the material are described using the Havriliak–Negami model according to Eq. (5) (Havriliak and Negami, 1966) and the relationship of Poisson's ratio [Eq. (6)] from the National Cooperative Highway Research Project's *Guide for Mechanistic-Empirical Design* (NCHRP, 2004),

$$E^* = E_\infty + \frac{(E_0 - E_\infty)}{[1 + (i\omega\tau)^\alpha]^\beta}, \tag{5}$$

where E_0 is the low frequency modulus (Pa), E_∞ is the high frequency modulus (Pa), α governs the frequency dependency, β governs the asymmetry of the loss peak, τ is the relaxation time (s), i is the complex number, and $\omega = 2\pi f$ where f is the frequency (Hz);

$$\nu = 0.15 + \frac{0.35}{1 + e^{(a+b\times\log(|E^*|))}}, \tag{6}$$

where a and b are material constants.

The Havriliak–Negami model has been chosen instead of the sigmoidal function, commonly applied to asphalt concrete (Brown *et al.*, 2009), due to the model's ability to characterize the complex modulus. The sigmoidal function describes only the dynamic modulus and is therefore not able to characterize the complete viscoelastic behavior of the material (Yusoff *et al.*, 2011). Furthermore, the Havriliak–Negami model can account for an asymmetrical loss peak and has proven to be very accurate in modeling the behavior of viscoelastic materials (Hartmann *et al.*, 1994; Madigosky *et al.*, 2006). Another important advantage with the Havriliak–Negami model is that is has relatively few parameters to estimate in an optimization process compared to other models commonly applied to asphalt concrete (Yusoff *et al.*, 2011).

A convergence study of the finite element model was performed to determine a sufficient maximum element size for good accuracy and to minimize the computational time. Figure 6 presents the finite element simulation of different mesh sizes for the fourth resonance frequency of the longitudinal vibration mode. The fourth resonance is presented because it is more sensitive to the mesh size than the lower resonance frequencies. In Fig. 6, it can be seen that results converges at a mesh size of 2 cm (2455 number of elements). The mesh of the finite element model (shown in Fig. 7) was built up by tetrahedral elements with quadratic shape functions.

The frequency response simulation of the specimen was performed by applying a unit force (1 N) in the x direction (see Fig. 7) at the center point of the y-z plane (0, 29.37, 29.47 mm). The force was applied over a frequency range of 100–20 000 Hz in steps of 20 Hz. The response of the simulation was obtained from the center point 382, 29.37, 29.47 mm. These points of the specimen correspond to the real load impulse and where the accelerometer was attached in the real measurements.

D. Optimization of the frequency response functions

The time-temperature superposition principle (TTSP) allows results from measurements at different temperatures and frequencies to be shifted to a single master curve expressed at a specific reference temperature or reference frequency (Brown *et al.*, 2009). Materials to which the TTSP can be applied are classified as thermorheological simple materials. In the Havriliak–Negami model, it is assumed that

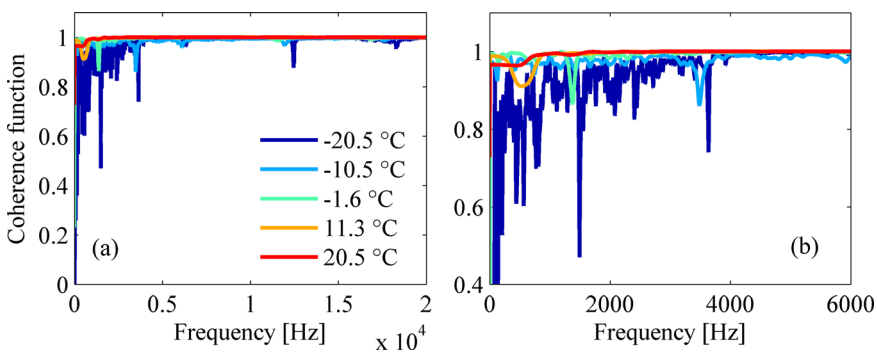

FIG. 5. (Color online) The coherence function of the measured FRFs (a) and a zoom of the lower frequency area (b).

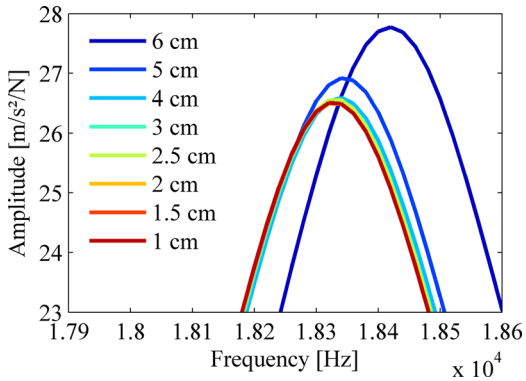

FIG. 6. (Color online) Convergence study of the finite element mesh.

the relaxation time (τ) is the only temperature dependent parameter (Madigosky *et al.*, 2006). This means that if the material is thermorheologically simple, the relaxation time is the only parameter that needs to be determined uniquely for each tested temperature. All other parameters in the Havriliak–Negami model should be able to be estimated to the same value for each temperature if the TTSP is applicable. Therefore theoretical FRFs are optimized against all measured FRFs simultaneously to estimate the complex modulus master curve through one single simulation. This is performed by substituting the Williams–Landel–Ferry equation [Eq. (7)] into the Havriliak–Negami model [see Eq. (8)]. By this, the shift factors allow the relaxation time (τ) to be unique for each temperature while all other parameters take the same values for all temperatures. A similar approach has been applied by Ren *et al.* (2011),

$$\log\alpha_T(T) = \frac{-c_1(T - T_{ref})}{c_2 + T - T_{ref}}, \tag{7}$$

where $\alpha_T(T)$ is the shift factor, T is the test temperature, T_{ref} is the reference temperature, and c_1 and c_2 are material constants (Williams *et al.*, 1955),

$$E^* = E_\infty + \frac{(E_0 - E_\infty)}{[1 + (i\omega\alpha_T(T)\tau)^\alpha]^\beta}. \tag{8}$$

The FRF optimized complex modulus master curve is in this paper also compared to complex moduli results obtained through optimizing the FRFs separately by estimating the four parameters E_∞, α, β, and τ for each test temperature [using Eq. (5)]. This comparison is performed to investigate the accuracy of the estimated master curve against results of the best possible matches of measured and theoretical FRFs.

MATLAB and the finite element program COMSOL MULTIPHYSICS 4.2 were used to perform the optimization of the FRFs. The frequency response simulations in the finite element program were combined with the *patternsearch* function in MATLAB, allowing an update of the model parameters by minimizing the error between the measured and theoretical FRFs. The *patternsearch* function has been found to be efficient in finding the global minimum for optimization of FRFs (Ren *et al.*, 2011). The following objective function [Eq. (9)] was used for the optimization of the FRFs, where the normalized measured FRF were used to weigh frequencies around the resonance peaks of the specimen higher. Other objective functions were also tested for the optimization process leading to similar results. The error was calculated for 60 points (frequencies) distributed over the three first resonance frequencies of the FRFs,

$$\text{Error} = \sum_{i=1}^{N}\left(|H_{MNorm_i}| \times \left|\frac{|H_{M_i}| - |H_{T_i}|}{|H_{M_i}|}\right|\right), \tag{9}$$

where H_{MNorm} = normalized measured frequency response function, H_M = measured frequency response function, H_T = theoretical frequency response function, N = number of data points, and i = index of the data point.

III. RESULTS AND DISCUSSIONS

A. Validation of the FEM optimization method

The method of optimizing FRFs was first applied to a PVC-U beam for measurements performed at a temperature of 21 °C. The reason for using a PVC-U specimen as validation of the method is that the material is homogenous with a relatively small frequency dependency. The specimen was modeled by the following simple relationship,

$$E^* = E_1(1 + \eta i) \tag{10}$$

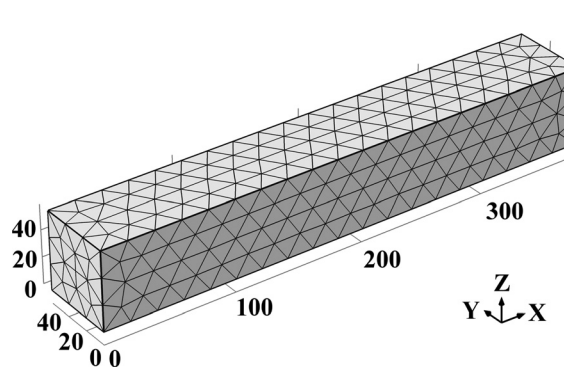

FIG. 7. The mesh of the finite element model.

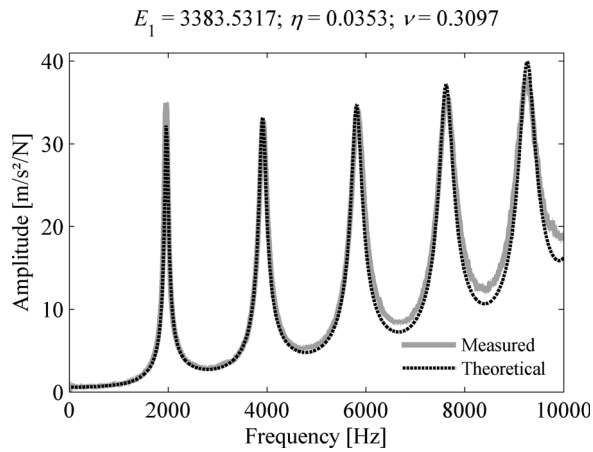

FIG. 8. The measured and fitted theoretical FRF of the beam shaped PVC-U specimen.

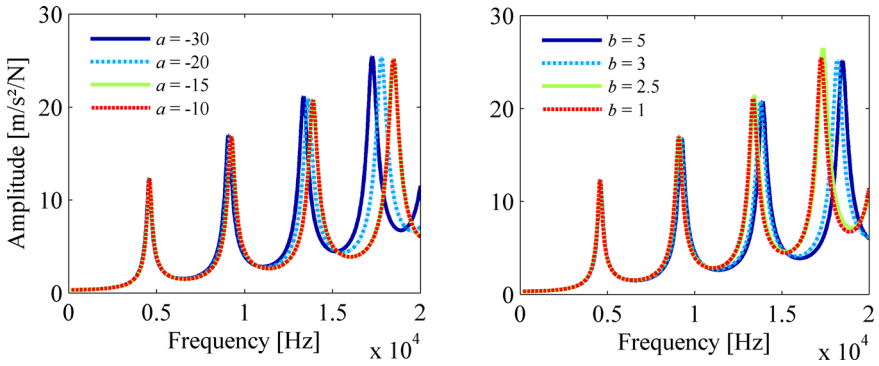

FIG. 9. (Color online) The influence of the parameters a and b in the relationship of Poisson's ratio [Eq. (6)] to the FRFs.

Values of the storage modulus (E_1), the loss factor (η), and Poisson's ratio (ν), giving the best possible match between the FRFs, were estimated in the optimization process. The match of the theoretical FRF of the PVC-U specimen to the measured FRF is presented in Fig. 8. The optimization of the FRF resulted in a dynamic modulus ($|E^*|$) of 3385.53 MPa and a Poisson's ratio of 0.31. This result is comparable to statically determined elastic moduli of PVC-U material reported in literature to be in the range of 2600 to 3300 MPa (Motavalli *et al.*, 1993).

B. Parameter analysis

Figure 9 presents a parameter analysis of Poisson's ratio where it can be seen that the FRFs at the lower half of the frequency range are not so sensitive to the coefficients a and b in the used Poisson's ratio relationship [Eq. (6)]. This may aggravate an accurate estimation of Poisson's ratio if a wider frequency range is not used to match the FRFs.

A parameter study of the low frequency modulus (E_0) showed that this parameter has a negligible influence of the FRFs for reasonable values of asphalt concrete. The low frequency modulus was therefore set to a fixed value of 100 MPa. This specific value is based on falling weight deflectometer measurements performed by Ullidtz *et al.* (2006), where the measurements resulted in a dynamic modulus higher than 100 MPa for all tested temperatures in field.

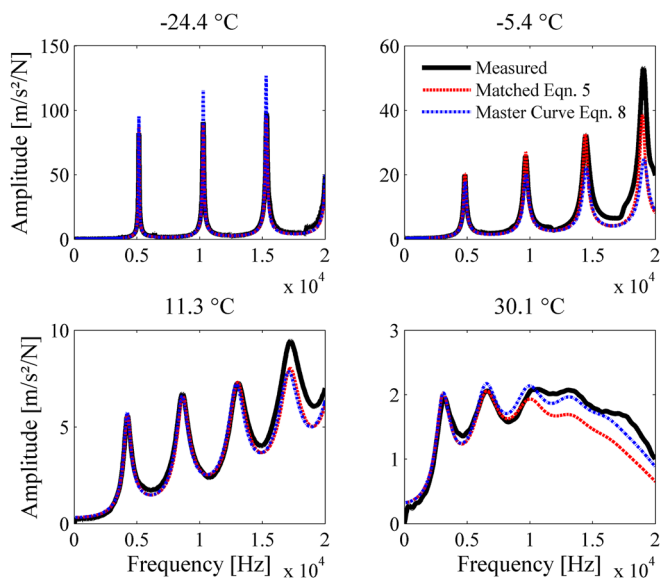

FIG. 10. (Color online) Measured and matched theoretical FRFs.

C. Results of the complex modulus and Poisson's ratio

Frequency ranges covering the three first resonance frequencies have been used to estimate the complex moduli at the different temperatures. However, the parameter study of the influence of Poisson's ratio to the FRFs showed that Poisson's ratio has a larger influence on higher resonance frequencies (Fig. 9). Thus using the three first longitudinal resonance frequencies was shown to not be enough to accurately evaluate the coefficients a and b in Eq. (6). These coefficients were therefore chosen to values of $a = -19$ and $b = 2.95$ (Gudmarsson *et al.*, 2012). These values might not provide the best possible match of the FRFs, but they give a reasonable estimation of Poisson's ratio. Moreover these fixed values still contribute to a good match between theoretical and measured FRFs (Fig. 10), which supports the previous approximation of the material constants a and b for this specimen.

Figure 10 shows the match of the optimized FRFs to the measured FRFs for four test temperatures. The figure presents the results of the directly estimated master curve through optimization of all FRFs simultaneously [Eq. (8)] as well as results of the FRFs optimized for each temperature separately [Eq. (5)]. A good match is seen especially for the individual optimized FRFs [Eq. (5)] but also the optimization of all FRFs simultaneously (Eq. (8)) shows a satisfying match. These results show that the optimization method can accurately describe the frequency dependent dynamic properties of an asphalt concrete specimen. Table II presents the resulting parameter values of the FRF optimized master curve using Eq. (8).

The resulting dynamic moduli (the absolute value of the complex moduli) based on optimizing the FRFs for each temperature separately [Eq. (5)] is presented in Fig. 11 along with the dynamic moduli determined using

TABLE II. Estimated master curve parameters through optimization of all FRFs simultaneously (where $E_0 = 100$ MPa, $a = 19$, $b = 2.95$ and $T_{ref} = 0\,^\circ$C).

Parameter	E_∞	α	β	τ	c_1	c_2
Value	37723e6	0.4239	0.3163	4.5072	14.9947	82.4206

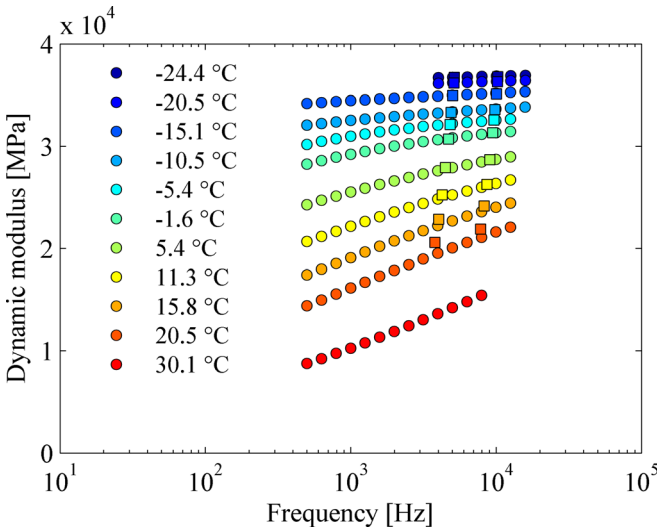

FIG. 11. (Color online) The results of the dynamic modulus using FRFs (○) and RAS (□).

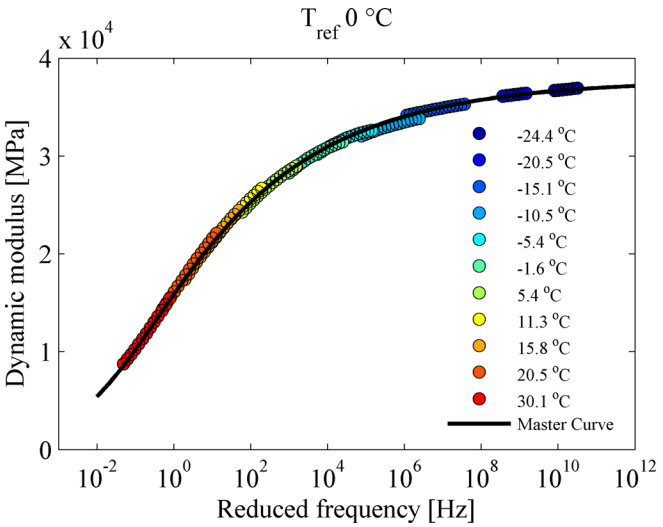

FIG. 12. (Color online) The dynamic modulus master curve determined through optimization of all FRFs simultaneously and the shifted dynamic moduli determined using optimization of the FRFs for each temperature separately.

RAS (Gudmarsson *et al.*, 2012). The FRFs optimized moduli are estimated over a frequency range of minimum 500 Hz to maximum 18000 Hz through the separately matched FRFs. Table III presents values of the dynamic modulus for some intermediate frequencies. A good agreement between optimization of FRFs and RAS are seen at lower temperatures. However, at higher temperatures, the agreement is worse. A reason for the difference between the methods at the higher temperatures could be due to limitations with the half-power bandwidth method. This method has been used to estimate the damping when applying RAS to a viscoelastic material (Gudmarsson *et al.*, 2012). Recent work by Wang *et al.* (2012) has showed that the half-power bandwidth method may overestimate the damping for multi-DOF systems. An overestimation of the damping leads to a higher modulus as can be seen in this case at the higher temperatures. Furthermore, Wang (2011) showed that the half-power bandwidth method is quite accurate for damping ratios less than 0.1 but that the accuracy of the method decreases with increasing damping ratios. Therefore the accuracy of the RAS determined moduli may decrease when the damping in the specimen increases with increasing temperatures. At the highest test temperature (30.1 °C), it was not possible to estimate the complex moduli using RAS due to the high damping in the material.

Figures 12 and 13 present the master curve determined by optimizing all FRFs at different temperatures simultaneously using Eq. (8) as well as the estimated moduli for each set of temperatures using Eq. (5) plotted against the reduced frequency. The master curve has been expressed over a frequency range of 10^{-2} to 10^{12} Hz. The dynamic modulus is shown in Fig. 12, and Fig. 13 shows the phase angle, which is defined as $\tan^{-1}$ of the ratio between the loss and storage modulus. A small deviation between the two optimization approaches can be seen in the two figures. This indicates that the asphalt concrete specimen has some degree of deviance from a complete thermorheologically simple behavior. However, the fit may be considered well enough for engineering applications in pavement management and design.

The Cole–Cole diagram (Fig. 14) emphasizes any differences between the two optimization methods because

TABLE III. The dynamic modulus (in MPa) for different frequencies and temperatures determined through optimization of each FRF separately.

f (kHz)\T(°C)	−24.4	−20.5	−15.1	−10.5	−5.4	−1.6	5.4	11.3	15.8	20.5	30.1
0.5	-	-	34177	32071	30183	28254	24262	20670	17392	14387	8729
1	-	-	34443	32524	30973	29218	25506	22160	19105	16129	10246
2	-	-	34685	32917	31595	30010	26618	23552	20730	17855	11886
3	-	-	34818	33124	31893	30404	27208	24316	21628	18841	12893
4	36687	36135	34909	33263	32080	30655	27602	24834	22237	19525	13626
6	36756	36219	35034	33446	32311	30973	28123	25530	23054	20462	14679
8	36805	36278	35120	33570	32456	31175	28468	26000	23604	21105	15436
10	36843	36324	35186	33662	32557	31321	28724	26350	24012	21590	-
12	36874	36362	35239	33736	32634	31432	28924	26628	24334	21978	-
14	36900	36394	35283	33796	32695	31521	29088	26857	24597	-	-
16	36923	36421	35322	33848	-	-	-	-	-	-	-
18	36923	36445	-	-	-	-	-	-	-	-	-

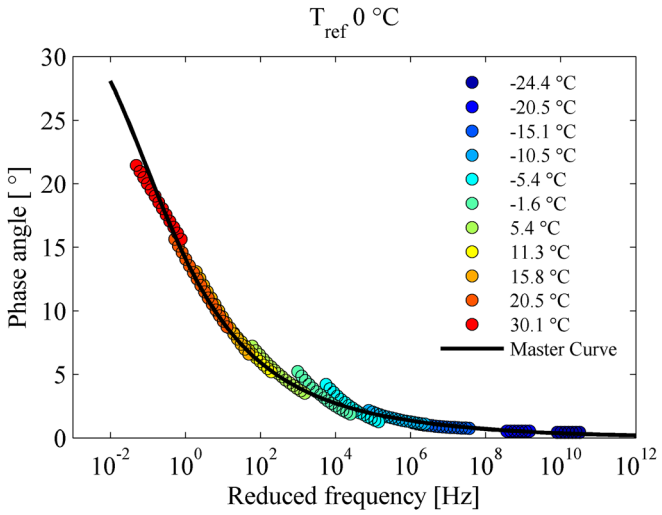

FIG. 13. (Color online) The phase angle master curve determined through optimization of all FRFs simultaneously and the shifted phase angle determined using optimization of the FRFs for each temperature separately.

this diagram is independent of any shift factors [Eq. (7)]. The results of the complex modulus at different frequencies and temperatures should all form a single curve in the Cole–Cole diagram if the material is thermorheologically simple (Cole and Cole, 1941; Levenberg, 2011). The Cole–Cole diagram of the complex moduli is a further indication of that constructing master curves using FRFs is a promising approach due to the relatively small deviation of the separately optimized FRFs to the FRF optimized master curve. The Cole–Cole figure also presents the results obtained by applying RAS to the same specimen. The difference (previously shown in Fig. 11) between the FRF optimization methods and RAS is highlighted in this figure. These results support the theory of the half-power bandwidth method being the reason for the deviation at higher temperatures between RAS and optimization of FRFs.

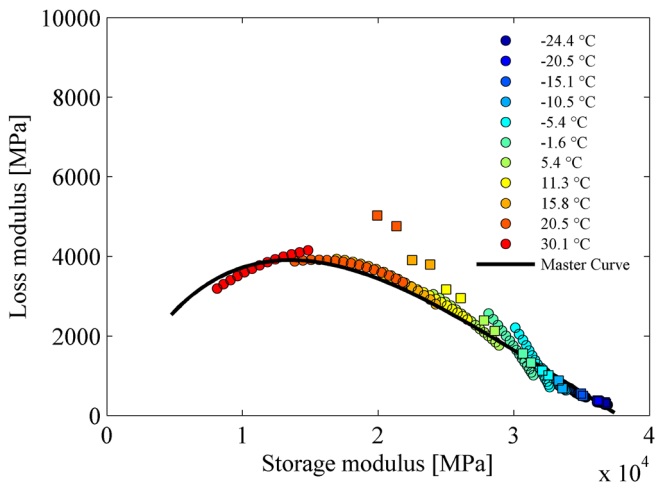

FIG. 14. (Color online) Cole–Cole diagram of the complex moduli determined for each temperature by optimizing the FRFs separately (○), determined by RAS (□), and by optimization all FRFs simultaneously (master curve).

IV. CONCLUSIONS

The method of optimizing FRFs is shown to be able to give a good fit between theoretical and measured FRFs and thereby accurately characterize the frequency dependent dynamic properties of an asphalt concrete specimen. The low strain complex modulus has been estimated over a frequency range of minimum 500 Hz to maximum 18000 Hz through the separately optimized FRFs. The FRF optimized master curve expresses the complex modulus over a wider frequency range, approximately between 10^{-2} and 10^{12} Hz. The separately estimated complex moduli are shown to have a relatively small deviation from a unique curve in the Cole–Cole space; this indicates that the method is promising in characterizing the master curve of an asphalt concrete specimen. The fixed values of the material constants of Poisson's ratio are an approximation that may be improved, although these values are shown to contribute to a good fit of the FRFs. An important benefit with the proposed FRF method is that it can be automated without any need for individual mode identification and also extend the frequency range used compared to the ASTM C215 standard and RAS.

ACKNOWLEDGMENTS

The Swedish transport administration and Swedish construction industry's organization (SBUF) are gratefully acknowledged for their financial support.

ASTM (**2008**). C215-08, *Standard Test Method for Fundamental Transverse, Longitudinal, and Torsional Frequencies of Concrete Specimens* (American Society for Testing and Materials, West Conshohocken, PA).

Brown, E. R., Kandhal, P. S., Roberts, F. L., Kim, Y. R., Lee, D. Y., and Kennedy, T. W. (**2009**). *Hot Mix Asphalt Materials, Mixture Design and Construction* (NAPA Reasearch and Education Foundation, Lanham, MD).

Buchanan, J. L. (**1987**). "Numerical solution for the dynamic moduli of a viscoelastic bar," J. Acoust. Soc. Am. **81**, 1775–1786.

Cole, K. S., and Cole, R. H. (**1941**). "Dispersion and absorption in dielectrics. I. Alernating current characteristics," J. Chem. Phys. **9**, 341–351.

COMSOL MULTIPHYSICS (**1998**). Version 4.2.

Gudmarsson, A., Ryden, N., and Birgisson, B. (**2012**). "Application of resonant acoustic spectroscopy to asphalt concrete beams for determination of the dynamic modulus," Mater. Struct., DOI:10.1617/s11527-012-9877-3.

Guo, Q., and Brown, D. A. (**2000**). "Determination of the dynamic elastic moduli and internal friction using thin resonant bars," J. Acoust. Soc. Am. **108**(1), 167–174.

Halvorsen, W. G., and Brown, D. L. (**1977**). "Impulse technique for structural frequency response testing," J. Sound Vib. Nov. 1977, pp. 8–21.

Hartmann, B., Lee, G. F., and Lee, J. D. (**1994**). "Loss factor height and width limits for polymer relaxations," J. Acoust. Soc. Am. **95**, 226–233.

Havriliak, S., and Negami, S. (**1966**). "A complex plane analysis of α-dispersions in some polymer systems," J. Polym. Sci. C **14**, 99–117.

Kweon, G., and Kim, Y. R. (**2006**). "Determination of the complex modulus of asphalt concrete using the impact resonance test," J. Transp. Res. Board **1970**, 151–160.

Lacroix, A., Kim, Y. R., and Far, M. S. S. (**2009**). "Constructing the dynamic modulus mastercurve using impact resonance testing," Assoc. Asph. Paving Technol. **78**, 67–102.

Leisure, R. G., and Willis, F. A. (**1997**). "Resonant ultrasound spectroscopy," J. Phys.: Condens. Matter **9**, 6001–6029.

Levenberg, E. (**2011**). "Smoothing asphalt concrete complex modulus test data," ASCE J. Mater. Civ. Eng. **23**(5), 606–611.

Madigosky, W. M., Lee, G. F., and Niemiec, J. M. (**2006**). "A method for modeling polymer viscoelastic data and the temperature shift function," J. Acoust. Soc. Am. **119**, 3760–3765.

Migliori, A., and Sarrao, J. L. (**1997**). *Resonant Ultrasound Spectroscopy–Applications to Physics, Materials Measurements and Nondestructive Evaluation* (Wiley–Interscience Publication, New York).

Motavalli, M., Farshad, M., and Flüeler, P. (**1993**). "Buckling of polymer pipes under internal pressure," Mater. Struct. **26**, 348–354.
NCHRP (**2004**). "Material characterization," in *Guide for Mechanistic-Empirical Design, Final Report. Part 2. Design Inputs* (National Cooperative Highway Research Project, St. Paul, MN), Chap. 2.
Ostrovsky, L., Lebedev, A., Matveyev, A., Potapov, A., Sutin, A., Soustova, I., and Johnson, P. (**2001**). "Application of three-dimensional resonant acoustic spectroscopy method to rock and building materials," J. Acoust. Soc. Am. **110**(4), 1770–1777.
Pasqualini, D. (**2006**). "Intrinsic nonlinearity in geomaterials: Elastic properties of rocks at low strain," in *Universality of Nonclassical Nonlinearity Applications to Non-Destructive Evaluations and Ultrasonic*, edited by P. P. Delsanto (Springer Science and Business Media, New York), pp. 417–423.
Ren, Z., Atalla, N., and Ghinet, S. (**2011**). "Optimization based identification of the dynamic properties of linearly viscoelastic materials using vibrating beam technique," ASME J. Vib. Acoust. **133**(4), 041012.
Renault, A., Jaouen, L., and Sgard, F. (**2011**). "Characterization of elastic parameters of acoustical porous materials from beam bending vibrations," J. Sound Vib. **330**, 1950–1963.
Rupitsch, S. J., Ilg, J., Sutor, A., Lerch, R., and Döllinger, M. (**2011**). "Simulation based estimation of dynamic mechanical properties for viscoelatic materials used for vocal fold models," J. Sound Vib. **330**, 4447–4459.
Ryden, N. (**2011**). "Resonant frequency testing of cylindrical asphalt samples," Eur. J. Environ. Civ. Eng. **15**, 587–600.
Trafikverket (**2009**). "VVTBT Bitumenbundna lager 09" ("VVTBT Bituminous layers 09"), Publication 2009:140, Borlänge, Sweden.
Ullidtz, P., Harvey, J., Tsai, B.-W., and Monismith, C. (**2006**). "Calibration of CalME models using WesTrack performance data," Report No. UCPRC-RR-2006-14 (Pavement Research Center, University of California, Berkley, CA).
Wang, I. (**2011**). "An analysis of higher order effects in the half power method for calculating damping," J. Appl. Mech. **78**, 014501.
Wang, J.-T., Jin, F., and Zhang, C.-H. (**2012**). "Estimation error of the half-power bandwidth method in identifying damping for multi-DOF systems," Soil Dyn. Earthquake Eng. **39**, 138–142.
Whitmoyer, S. L., and Kim, Y. R. (**1994**). "Determining asphalt concrete properties via the impact resonant method," J. Test. Eval. **22**(2), 139–148.
Williams, M. L., Landel, R. F., and Ferry, J. D. (**1955**). "The temperature dependence of relaxation mechanisms in amorphous polymers and other glass-forming liquids," J. Am. Chem. Soc. **77**, 3701.
Yusoff, N. I. Md., Shaw, M. T., and Airey, G. D. (**2011**). "Modelling the linear viscoelastic rheological properties of bituminous binders," J. Constr. Build. Mater. **25**(5), 2171–2189.